Université de Montréal

Biocompatible Polymer Coatings for Implants in the Peripheral Nervous System

In vivo study of polymer-coated microbeads in the rat sciatic model

Par

Vincent Weng-Jy Cheung

Département des sciences biomédicales, Faculté de médecine

Mémoire présenté en vue de l'obtention du grade de maîtrise

en sciences biomédicales, option médecine expérimentale

Août 2020

Université de Montréal

Département des sciences biomédicales, Faculté de médecine

Ce mémoire intitulé

Biocompatible Polymer Coatings for Implants in the Peripheral Nervous System

In vivo study of polymer-coated microbeads in rat sciatic model

Présenté par

Vincent Weng-Jy Cheung

A été évalué(e) par un jury composé des personnes suivantes

Bénédicte Amilhon
Président-rapporteur

Jenny Catherine Lin
Directeur de recherche

Natalie Habra
Membre du jury

Résumé

Introduction: Les implants dans le système nerveux périphérique (SNP) peuvent potentiellement restaurer les capacités sensorielles et motrices chez les patients avec des amputations des membres supérieures. Cependant, la réaction à un corps étrangers affecte significativement la fonction à long-terme et la biocompatibilité de ces systèmes avec le temps. Le dendrimère (DND) et la Poly-D-Lysine (PDL) sont deux polymères synthétiques qui peuvent potentiellement améliorer la performance de ces implants. Pour cette étude, notre objectif est de déterminer si ces polymères peuvent promouvoir la formation d'éléments présynaptiques sur des surfaces synthétiques in vivo dans un modèle animal.

Méthodes: Pour l'étude in vivo, nous avons utilisé un modèle d'écrasement du nerf sciatique chez le rat. Des billes enduites de DND et PDL et contrôle ont été injectées dans le nerf sciatique aux sites d'écrasement et 5 mm distaux au site d'écrasement. Après 4, 6 et 8 semaines, les nerfs ont été retirés et marqués avec des anticorps spécifiques au neurofilament et à la synaptophysine. Nous avons ensuite compté le nombre d'éléments présynaptiques retrouvant sur la surface de chaque bille pour toutes les conditions. Pour l'étude de l'électrode, deux électrodes ont été implantées dans le nerf sciatique du rat. Nous avons ensuite effectué des enregistrements nerveux à chaque semaine, et le potentiel d'action dans le nerf a été mesuré en variant uniquement la largeur de l'impulsion.

Résultats: L'étude in vivo a démontré que les billes enduites de DND pouvaient promouvoir une accumulation significative de synaptophysine sur leurs surfaces comparé aux billes contrôles de 4 à 8 semaines. À 4 semaines, les billes dans la condition DND avaient également une accumulation de synaptophysine significativement supérieure à celles dans la condition PDL pour le site distal à l'écrasement. L'étude de l'électrode a démontré que les deux électrodes pouvaient stimuler et acquérir des signaux nerveux du nerf sciatique jusqu'à 1 et 2 semaines respectivement avant de ne plus fonctionner.

Conclusion: Les résultats de notre étude suggèrent que DND possède une propriété à promouvoir la synaptogenèse qui est supérieure à PDL in vivo et que notre modèle d'électrode peut être utilisé pour évaluer la stabilité du signal des implants SNP.

Mots-clés: Polymères synthétiques, Dendrimères, Réaction à corps étranger, Synaptophysine, Écrasement nerveux, Amputés, Lésions nerveuses périphériques, Électrodes, Lysine, Microsphères.

Abstract

Background: Implants in the peripheral nervous system (PNS) can potentially restore sensory feedback, improve motor control and alleviate phantom-limb pain in upper-limb amputees. However, nervous system implants have poor long-term function and biocompatibility when implanted into the body due to foreign body reaction. Dendrimer (DND) and Poly-D-Lysine (PDL) are two synthetic polymers with properties that could improve the performance of these interfaces. In my masters' research, my objective is to determine whether these synthetic polymers could promote the formation of presynaptic elements on artificial surfaces in vivo making intraneural implants more biocompatible and long-lasting.

Methods: In the coated microsphere in vivo experiment, a nerve crush injury model in the rat was used for the study. PDL-coated, DND-coated and uncoated beads were injected into the rat sciatic nerve at the crush site and 5 mm distal to the crush site. The nerves were then harvested after 4, 6 and 8 weeks and stained for neurofilament and synaptophysin. Synaptophysin puncta were then counted on the bead surface for each group. Additionally, in a proof-of-concept experiment, two uncoated electrodes were implanted into the rat sciatic nerve. Nerve recordings were then performed every week, and the threshold nerve potential in the sciatic nerve was measured by only varying the pulse duration of the stimulation.

Results: The coated microsphere in vivo experiment demonstrated that DND-coated microspheres had a significantly higher number of synaptophysin puncta around their surface from 4 to 8 weeks compared to uncoated beads. At 4 weeks, the DND condition also showed a significantly higher number of synaptophysin puncta around its microbeads vs. the PDL condition for the distal site. In the uncoated electrode in vivo experiment, the results showed that the two implants could stimulate and record threshold nerve potentials in the rat sciatic nerve for one week and two weeks respectively before being non-functional.

Conclusion: Our study showed for the first time that DND has a stable synapse-promoting property that is superior to PDL in vivo and that our electrode design can be used to assess the long-term signal stability of peripheral nerve implants.

Keywords: Synthetic Polymers, Dendrimers, Foreign Body Reaction, Microspheres, Synaptophysin, Nerve Crush, Amputees, Peripheral Nervous Injuries, Lysine, Intraneural Electrodes.

Table of Contents

Liste des tableaux

Liste des figures

Liste des sigles

°C: Celsius

kg: Kilogram

kDa: Kilodalton

mg: Milligram

ml: Milliliter

µl: Microliter

µm: Micrometer

nm: Nanometer

µA: Microampere

nC: Nanocoulomb

rpm: Revolutions per minute

Hz: Hertz

Liste des abréviations

AWG: American wire gauge

ANOVA: Analysis of Variance

BSA: Bovine Serum Albumin

CNS: Central Nervous System

CNTs: Carbon Nanotubes

CTRL: Control

DND: Dendrimer

DIV: Days In Vitro

DNA: Deoxyribonucleic Acid

EMG: Electromyography

FBR: Foreign Body Reaction

HSPGs: Heparan Sulfate Proteoglycans

ITO: Indium Tin Oxide

IPSC: Induced Pluripotent Stem Cells

IML: Innate Molecular Layer of the Dental Gyrus

NSAIDs: Nonsteroidal Anti-inflammatory Drugs

OCT: Optimal Cutting Temperature

PAMAM: Polyamidoamine

PEI: Poly(propylene) Imine

PBS: Phosphate-buffered Saline

PLL: Poly-L-Lysine

PDL: Poly-D-Lysine

PFA: Paraformaldehyde

PNS: Peripheral Nervous System

PLS: Phantom-Limb Syndrome

Pt/Ir: Platinum/Iridium

RIM: rab3a-interacting Molecule

SEM: Standard Error of the Mean

SNR: Signal-to-Noise Ratio

SSBLMs: Spherical Supported Bilayer Lipid Membranes

TCAs: Tricyclic Anti-Depressants

TENS: Transcutaneous Nerve Stimulation

TMS: Transcranial Magnetic Stimulation

TMR: Targeted Muscle Reinnervation

VAChT: Vesicular Acetylcholine Transporter

Remerciements

Dre. Jenny Catherine Lin, pour m'avoir donné l'opportunité de compléter ma maîtrise dans son laboratoire, m'avoir autorisé à assister à ses cliniques et m'avoir aidé tout au long de mon parcours à la maîtrise à travers ses conseils et son leadership.

Dr. Timothy Edward Kennedy, pour m'avoir autorisé à utiliser les instruments et les matériels dans son laboratoire et m'avoir dirigé dans une bonne direction par ses conseils et sa rigueur scientifique.

Dre. Xiya Ma, pour m'avoir aidé tout au long de mon parcours à la maîtrise à travers ses conseils, m'avoir présenté aux chercheurs pouvant m'aider dans mon projet, m'avoir enseigné les techniques pour le projet et m'avoir aidé dans l'analyse de données.

Michel Paquet, pour m'avoir enseigné les techniques chirurgicales et de laboratoire nécessaires pour compléter les études dans mon projet, m'avoir aidé à la réalisation des études et m'avoir donné des conseils sur l'enregistrement électrophysiologique et l'analyse de données.

Timothy Lan Chun Yang, pour m'avoir aidé tout au long de mon parcours à la maîtrise et m'avoir assisté dans les chirurgies et les études dans le projet.

Jean-Pierre Clément, pour m'avoir donné des conseils sur le marquage d'anticorps et l'analyse de données et m'avoir fourni les matériels nécessaires pour compléter le projet.

Dre. Maran Ma, pour m'avoir aidé avec le système d'enregistrement électrophysiologique, m'avoir assisté dans l'acquisition et le traitement de données et m'avoir donné des conseils sur la conception de l'électrode.

Dr. Daryan Chitsaz, pour m'avoir donné des conseils sur la microscopie et sur l'analyse de données.

Mon entourage, pour m'avoir supporté pendant ces deux dernières années avec leur encouragement et leur attitude positive.

Chapter 1 – Introduction

.1 Introduction

.1.1 Clinical Context

In the United States, limb-loss affected more than 500 000 people in 2005 and is projected to affect 2.2 million people in 2020 (Ziegler-Graham et al., 2008). Upper-limb amputation can cause severe disabilities in patients, such as significant motor and sensory loss. These abrupt changes in the life of upper-limb amputees can influence both their physical and mental well-being. A study conducted in Spain showed that only 51% of patients who suffered upper-limb amputation with an average age of 35 years old would eventually return to work (Fernández et al., 2000). Other studies have also reported that patients with upper-limb amputation were more likely to experience signs of depression and anxiety compared to the general population (Darnall et al., 2005; Desmond, 2007). The development of these affective conditions is a consequence of profound changes in body image and self-concept brought by the amputation injury. Moreover, diverse complications can develop after the amputation procedure, such as phantom-limb syndrome and neuromas. Neuromas often occur following a nerve injury where the damaged nerve fibers are regenerating in an unorganized manner forming an aggregate of axons and non-neuronal cells (Zabaglo et al., 2020). These clinical conditions can inflict tremendous chronic pain and psychological distress to patients aside from the disability itself (Bhuvaneswar et al., 2007). Therefore, upper-limb amputation can have a significant impact on the quality of life of patients.

.1.2 Current Upper-limb Prosthetics

.1.2.1 Currently available upper limb prostheses and their drawbacks

A range of prosthetic devices has been developed over the years for the treatment of upper-limb amputation. The existing types of prostheses include passive, body-powered, myoelectric and hybrid prostheses. The most sophisticated systems presently on the market are myoelectric systems (Smail et al., 2020). They are externally powered devices that use residual EMG activity from surface sensors on stump muscles to control a prosthetic arm. Although myoelectric systems

can replace some upper-limb functions in amputees, the main limitation with these devices is the lack of sensory feedback and precise motor control of the prosthetic. The absence of these two crucial functionalities causes the control of myoelectric systems to be less intuitive and more challenging for patients. The lack of sensory feedback from currently available upper limb prostheses results in users having to rely continually on visual feedback to operate their prosthetic devices. When patients do not have visual feedback, they have to depend on the vibrations of their socket or the sounds of the motors to complete the tasks (Graczyk et al., 2018). This lack of sensory feedback makes it difficult to manipulate objects as no sensations are triggered in the hand. These considerations are cognitively demanding and ineffective for the control of upper-limb prosthetics (Lewis et al., 2012).

Moreover, limb loss eliminates many crucial muscle groups available for the control of the prosthetic hand (Ciancio et al., 2016). As a result, upper-limb amputees have to depend on the remaining muscle activity in the residual limb to replace all the ones lost in the amputation (Kuiken et al., 2017). This limited muscle availability affects the dexterous control of myoelectric devices and prevents users from performing the movements that they desire. In the clinical context, this could translate to prolonged training time and reduced performance on complex tasks (Ciancio et al., 2016). The elevated abandonment rate of these devices (up to 75%) suggests that myoelectric systems do not satisfy the functional needs and expectations of patients with upper-limb amputation (Biddiss et al., 2007). For example, users find it more convenient to use their contralateral intact arm to complete a task rather than their prosthetic hand. The frustration associated with current upper-limb devices suggests that we need to develop novel strategies to integrate sensory feedback and provide better motor control.

.1.3 Peripheral Nervous System

.1.3.1 The anatomy and structure of peripheral nerve

The peripheral nerve is the basic unit that allows for the function of the PNS (Krassioukov, 2002). It is formed from a combination of myelinated and unmyelinated nerve fiber bundles. These nerve bundles, or fascicles, are enveloped by a collagenous membrane, called the endoneurium. These endoneurium-sheathed fascicles are then grouped and surrounded by loose connective tissue,

called the perineurium. The entire nerve is then covered by the epineurium, a membrane composed of fibrocytes and collagen fibers. These membrane layers help to protect and confer strength and flexibility to the peripheral nerves (Krassioukov, 2002).

.1.3.2 The anatomy and structure of PNS

The peripheral nervous system comprises the axons and ganglions that are outside of the central nervous system (brain and spinal cord). It has the critical functions of maintaining homeostasis and mediating locomotion and sensation (Romero-Ortega, 2014). The two main nerve pathways in the PNS are the afferent and efferent pathways. The afferent pathway relays sensory information, such as temperature and proprioception, from the peripheral receptors to the CNS (Krassioukov, 2002). The efferent pathway transmits motor commands from the CNS to the muscles, allowing the body to interact with the environment (Krassioukov, 2002). This closed-loop system allows us to continuously mediate sensory feedback and motor function allowing for precise and intuitive movements. To reproduce this complex system, an artificial prosthetic arm would need a bidirectional interface that can process both motor and sensory signals.

.1.4 Peripheral Nerve Implants

.1.4.1 The potential applications of peripheral nerve implants

The use of peripheral nerve implants in the PNS is becoming a relevant field of research for the restoration of sensory feedback and motor control for upper-limb prosthetic devices. Peripheral nerve implants are electrode interfaces inserted into the PNS that can stimulate and acquire nerve signals from peripheral neurons. Studies have demonstrated that such devices can trigger certain sensations, such as vibration and pressure, at various locations of the patient's phantom limb (Davis et al., 2016; Dhillon & Horch, 2005; Petrini et al., 2019; Tan et al., 2014). These results suggest that electrode interfaces may help restore sensory feedback to amputees through electrical stimulation. Moreover, experiments have also demonstrated that peripheral nerve implants may help the management of various complications associated with upper-limb amputation, such as phantom-limb pain (Dhillon, Kruger, et al., 2005; Tan et al., 2014). These findings suggest that peripheral nerve implants may have the potential to considerably improve patient outcomes and the adoption rate of electric prosthetics in upper-limb amputees.

.1.4.2 Regenerative electrodes

A variety of peripheral nerve implants have been developed over the years for the restoration of sensory feedback. The existing types of peripheral systems are regenerative, extrafascicular and intrafascicular electrodes (Rijnbeek et al., 2018). Regenerative electrodes are implants that have a scaffold supporting axonal regeneration (Rijnbeek et al., 2018). Some of these devices have micropores that allow the separation of the regenerating nerve into sensory and motor fibres. Others contain chemical factors that attract or repel some types of peripheral neurons allowing for more selective stimulation of the nerve. These advantageous features have led to extensive research being completed on regenerative implants.

.1.4.3 Extrafascicular electrodes

Extrafascicular (or extraneural) electrodes are implants that wrap around the outer membrane of the nerve, called the perineurium. The superficial positioning of the device reduces the invasiveness of the implantation surgery. Studies have used cuff electrodes (Zollo et al., 2019) and flat-interface nerve electrodes (FINEs) (Schiefer et al., 2016; Tan et al., 2014) to restore sensory feedback in upper-limb amputees. A limitation of these systems is that they can only deliver electrical stimulations on the surface of the nerve. As a result, a higher level of stimulation is required to trigger a response in the peripheral neurons. These systems also have a lower selectivity compared to intraneural implants.

.1.4.4 Intrasfascicular electrodes

Intrafascicular (or intraneural) electrodes are interfaces implanted directly into the nerve fascicles. The proximity of the contact sites with the axons allows for selective activation of the individual nerve fibres. The stimulation amplitude required to trigger a nerve response is also lower compared to the extraneural systems. Many studies have used longitudinal intrafascicular electrodes (LIFEs) (Rossini et al., 2010), transverse intrafascicular multichannel electrodes (TIMEs) (D'Anna et al., 2019; Granata et al., 2018; Oddo et al., 2016; Petrini et al., 2019; Raspopovic et al., 2014) and Utah slanted electrode arrays (USEAs) (George et al., 2019; Page et al., 2018; Wendelken et al., 2017) in patients with upper-limb amputation. Although these devices require an invasive implantation procedure, this type of implant has been extensively tested and used in

experiments to restore sensory feedback and motor functions in patients with upper-limb amputation.

.1.5 Restoration of Sensory Feedback

.1.5.1 The conventional methods for the restoration of sensory feedback

Different strategies have been developed for the restoration of sensory feedback in myoelectric systems. These include vibrotactile, electrotactile, mechanotactile stimulation and targeted sensory reinnervation (Ciancio et al., 2016). Although these approaches have had some success in upper-limb amputees, conflicting findings have arisen concerning the actual benefits of these techniques for the intuitive control of myoelectric prosthetics. Some studies suggest that these methods do not considerably improve the functional performance of hand prosthetics in certain experimental conditions (Brown et al., 2015; Markovic et al., 2018; Raveh et al., 2018). Therefore, groups have explored other techniques to restore sensory functions in patients.

.1.5.2 The restoration of sensory feedback using peripheral nerve implants

Preliminary studies have used peripheral nerve implants as a bidirectional system to restore sensory feedback in patients with upper-limb amputation. Although requiring invasive surgery, peripheral nerve implants can restore the natural sensations evoked in the intact human hand (Valle et al., 2018). This is possible because motor and sensory pathways in an amputated arm can have residual neural activity after even 30 years (Dhillon & Horch, 2005). However, this approach requires a prosthetic arm equipped with tactile and proprioceptive sensors that can detect various afferent stimuli, like pressure and vibration (Ciancio et al., 2016). The system also needs to be able to encode these signals into electrical stimulation that the peripheral nerve implant can use to activate sensory nerve pathways. Studies have shown that the activation of the median and ulnar nerves using electrode microarrays triggered various sensations in a patient's phantom limb, such as tingle, vibration, brushing and pressure (Davis et al., 2016; George et al., 2019; Tan et al., 2015; Wendelken et al., 2017). These perceived sensations provided the user with information about the environment and their prosthetic arm helping them adjust their movements when completing a task (Ciancio et al., 2016). With sensory feedback, the

control of the prosthetic arm feels more intuitive, and thereby increasing the duration during which patients wore their hand prosthetic and used it to complete tasks (Graczyk et al., 2018).

.1.5.3 Patient outcomes with sensory feedback under experimental conditions

Peripheral nerve implants have been shown to reliably restore sensory feedback in patients with upper-limb amputation under experimental conditions. Through complex encoding strategies, intraneural electrodes have allowed upper-limb amputees to regain crucial sensory features, such as grip control (Petrini et al., 2019), slippage detection (D'Anna et al., 2019), and object and texture discrimination (George et al., 2019; Oddo et al., 2016; Raspopovic et al., 2014). Moreover, the restoration of a healthy representation of the phantom limb improved the psychosocial aspects of the disability. In studies, upper-limb amputees have reported improved prosthetic embodiment, body image and quality of life due to the restoration of sensory feedback (Graczyk et al., 2018; Page et al., 2018; Valle et al., 2018). Patients have also reported higher satisfaction after receiving sensory stimulation using peripheral nerve implants (Graczyk et al., 2018; Tan et al., 2014; Wendelken et al., 2017). The proper integration of sensations in the prosthetic arm translated to better performance on complex tasks for patients. For example, upper-limb amputees had a higher success rate when plucking a stem from a cherry using a prosthetic device with sensory feedback. The subjects also felt more confident and less distracted when completing these diverse tasks (Graczyk et al., 2018; Schiefer et al., 2016; Tan et al., 2014; Valle et al., 2018). These findings suggest that peripheral nerve implants can improve long-term prosthetic use and provide intuitive control through sensory feedback (Raspopovic et al., 2014).

.1.6 Restoration of Motor Control

.1.6.1 The conventional myoelectric prosthetic and TMR

Diverse strategies have been developed for the restoration of intuitive motor control in patients with upper-limb amputation. The conventional approach for treating motor deficits in patients is through myoelectric prosthetics. These systems use the agonist and antagonist muscles of the patient to control the opening and closing of a prosthetic hand (Cheesborough et al., 2015). Although myoelectric systems are successfully used in patients with upper-limb amputation, their motor control is usually limited to one movement at a time (Dhillon et al., 2004). They also require

the patient to co-contract their muscles to switch between the different grips of the hand prosthetic. As a result, these repeated contractions and stimulations of the muscle can lead to muscle fatigue, and their performance is highly dependent on environmental factors (Cracchiolo et al., 2020). The patient outcome also varies significantly depending on the type of muscles that were spared by the amputation surgery. For example, restoration of motor activity for proximal amputations can be extremely challenging due to the lack of usable motor sites for the prosthetic arm. A recent approach that was developed to improve myoelectric prosthetic function is targeted muscle reinnervation (TMR) (Cheesborough et al., 2015). This technique consists of transferring nerves associated with the amputated limb of the patient onto the residual and functional muscles of the stump. The reinnervated muscles then serve as an amplifier for the neural activity of the nerve. As a result, this procedure increases the number of control sites that can be used by the patient to control a multi-joint robotic arm, allowing them to perform multiple movements at once. However, the success of the surgery and the performance of the prosthetic arm depend on the length of the available nerve and the level of the amputation.

.1.6.2 The restoration of motor control using peripheral nerve implants

An alternative approach to restore motor control would be to use intraneural electrodes to interface with the sensory and motor nerve pathways of the patient's residual limb. This strategy provides higher selectivity and recording capabilities compared to surface EMGs (Cracchiolo et al., 2020). So far, most of the work completed on peripheral nerve implants has been focused on the restoration of sensory feedback as discussed previously. In comparison, little research has been done on using these interfaces for the restoration of motor control in upper-limb amputees. However, some studies have suggested that residual motor information remains in the nerve after an amputation injury (Dhillon et al., 2004; Kuiken et al., 2017). For example, a patient was able to generate motor activity in the nerve pathways for his missing limb after a 29-month amputation injury (Eggers et al., 2018). Similar results were also observed for subjects with above- and below-elbow amputations (Dhillon et al., 2004). These findings suggest that it would be possible to use peripheral nerve implants to extract and use motor information from the amputated nerve stumps to restore precise motor control in patients. Further evidence supporting this idea comes from studies showing that upper-limb amputees could use motor

intentions in the nerve to control the finger position of a virtual arm and the grip strength and elbow position of a robotic arm (Davis et al., 2016; Dhillon & Horch, 2005; Wendelken et al., 2017). For some of these systems, the control of a hand prosthetic increased up to 5 degrees of freedom, and the time required for the training sessions was reduced compared to surface EMGs (Wendelken et al., 2017). These findings suggest that peripheral nerve implants may be a more suitable choice compared to myoelectric prosthetics and TMR for the restoration of dexterous control in upper-limb amputees.

.1.7 Phantom-Limb Syndrome

.1.7.1 The cause of PLS

Phantom limb pain is a common complication found in upper-limb amputation. This condition affects up to 80% of patients with upper-limb amputation (Dhillon, Kruger, et al., 2005). After amputation surgery, these patients experience painful sensations at the level of their phantom limb (Maduri et al., 2020). Studies suggest that these symptoms occur primarily due to the reorganization in the primary somatosensory and motor cortex (Baron et al., 2010; Dickinson et al., 2010; Ramachandran et al., 2010). In the absence of sensory stimulus from the nerve pathways to the phantom limb, the representation of the cortical regions becomes abnormal as the hand motor area decreases in size compared to the contralateral hand area. This observation is the outcome of the neighbouring cortical areas taking over the hand representation area (Subedi et al., 2011). Significant molecular changes also occur in other parts of the body, such as the stump, spinal cord, brainstem and thalamus (Kaur et al., 2018; Maduri et al., 2020). Although many mechanisms have been proposed, the process of PLS is still under research. The present management options for phantom-limb pain are limited mostly to neuropathic pain medications, tricyclic anti-depressants (TCAs), acetaminophen, opioids, and nonsteroidal anti-inflammatory drugs (NSAIDs) (Kaur et al., 2018; Maduri et al., 2020). However, these treatments are only effective in providing temporary pain relief to upper-limb amputees. Other non-pharmacological treatments include mirror therapy, mental imagery and transcutaneous nerve stimulation (TENS).

.1.7.2 The treatment of PLS using nerve stimulation

Studies have shown that peripheral nerve stimulation could help patients re-establish a normal representation of their missing limb and alleviate the pain caused by the phantom-limb syndrome. In a study, two subjects reported a decreased frequency of pain episodes after sensory stimulation using a peripheral electrode (Tan et al., 2015). The representation of the missing limb in these patients also changed significantly after restoring sensory feedback. The subjects reported that the perception of their phantom limb returned to normal and was less painful or distorted (Horch et al., 2011; Page et al., 2018; Petrini et al., 2019; Valle et al., 2018). Others have reported that their phantom limb was opening up and that the fingers had more degrees of motion (Page et al., 2018). These improvements in PLS symptoms are a consequence of the anatomic and somatotopic changes in the CNS. The asymmetry in the hand motor area associated with the phantom limb was considerably reduced after 4 weeks of sensory stimulation using an intraneural electrode (Rossini et al., 2010). These studies suggest that peripheral nerve implants could serve as an alternative treatment option for pain medications in phantom-limb pain.

.1.8 Foreign Body Reaction

.1.8.1 The foreign body reaction process

Peripheral nerve implants may be useful for restoring sensory feedback, providing more intuitive motor control, and possibly also help to alleviate phantom-limb pain in patients with an upper-limb amputation. However, one major limitation of these peripheral nerve implants is that they have reduced long-term signal stability and electrode function over time (Lotti et al., 2017). Intraneural electrodes have been commonly used for the study of the restoration of sensory feedback and motor control under experimental conditions. They are the preferred interfaces for the intuitive control of prosthetic arms because of their higher selectivity, better signal-to-noise ratio and lower stimulation levels compared to extraneural electrodes (de la Oliva, Mueller, et al., 2018). The only drawback of this type of implant is the invasive implantation procedure, which can cause significant damage to the nerves. The normal wound healing process is also greatly affected by the presence of the intraneural electrode (Lotti et al., 2017). As a result, foreign body reaction starts to develop in the body leading to prolonged inflammation at the site of injury.

Macrophages start to migrate to the damaged area and produce different active chemicals, such as growth factors and pro-inflammatory cytokines. These chemicals activate the recruitment of fibroblasts, which then form a thick capsule of scar tissue around the implant. The fibrous layer becomes larger and larger over time encapsulating and disrupting the contact sites of the electrode. This reaction can be exacerbated depending on the properties of the electrode surface of the peripheral nerve implant (Lotti et al., 2017).

.1.8.2 The effect of FBR on peripheral nerve implants

The developing scar tissue around implants can have significant effects on the long-term function of intraneural devices. For example, the electrical impedance of electrode sites can increase due to tissue scarring, and this can lead to electrode failure over time. This effect was demonstrated in a study where the impedance of an intraneural system implanted into rats increased slowly in the first month and remained stable afterwards (Petrini et al., 2019; Wurth et al., 2017). An enlargement of cells and collagen was also observed around the device in the first 3-4 weeks. The concomitant occurrence of these two events suggests that the formation of the fibrotic membrane played a significant role in affecting the electrical impedance of the peripheral nerve system. The secondary effect of FBR on peripheral nerve implants is the increase of stimulation levels required to trigger a nerve response in the PNS. This outcome is either in response to the encapsulating tissue or the higher electrical impedance of the recording electrodes, which degrades the signal stability of the system. In one study, a patient implanted with an intraneural electrode had to increase the minimum stimulation charge from 0.1 nC to 1 nC in the first 10 days after the implantation to feel any sensations in his phantom limb (Rossini et al., 2010). These studies show evidence that the foreign body reaction can reduce the long-term function of peripheral nerve implants. This loss of function has important implications for patients with an upper-limb amputation who depend on their implant for the control of a prosthetic arm. To make peripheral nerve implants a viable long-term solution for upper-limb amputation, researchers will have to develop technologies that will reduce the effect of FBR on the electrode surface.

.1.9 Synapse formation on microbeads in CNS studies

.1.9.1 Preliminary studies on microbeads

Several research groups have described the potential of inducing synapse formation onto artificial surfaces. Most of these experiments were completed in the CNS through the culture of microbeads onto cerebellar tissues (Richard W. Burry, 1980, 1982; Richard W. Burry, 1983; R. W. Burry et al., 1986). These studies suggested that a poly-basic compound or charge when coated onto the surface of microbeads could promote the formation of presynaptic elements at the contact sites between the cerebellar neurons and coated microbeads. An experiment supporting this finding tested the effect of various charged proteins on Sepharose beads by culturing them with rat cerebellum at 7 DIV (Richard W. Burry, 1980). Among the charged compounds examined, poly-L-lysine, poly-ornithine and cationized ferritin were shown to induce the formation of apparent presynaptic elements within neuronal swellings after 24 hours of culture. This result was found through the observation of synaptic vesicles within newly-formed neuronal swellings in contact with cationized ferritin coated microbeads under the electron microscope. As observed through higher magnification electron micrographs, the synaptic vesicles had a diameter of approximately 40 nm and an electron dense material around their surface confirming them to be presynaptic elements (Richard W. Burry, 1980). In contrast, weaker basic compounds, such as spermidine, putrescine and cytochrome C, did not show any of these results. This study suggested that poly-basic compounds were necessary for the mechanism of synapse formation.

.1.9.2 In vitro and vivo studies in rat cerebellum

The important implications of a study showing that poly-basic compounds are important for presynaptic formation have pushed for more research to be completed on poly-L-Lysine (PLL) and poly-ornithine (Richard W. Burry, 1980). Another experiment completed by the same group demonstrated that PLL-coated microbeads could induce the formation of apparent presynaptic elements within 2 hours of culture in rat cerebellum (Richard W. Burry, 1982). These presynaptic complexes were also shown to be positive-labelled with SV48 and Synapsin I and to have 50-nm diameter synaptic vesicles (R.W. Burry et al., 1986). However, the number of presynaptic elements was decreased at 5 and 9 days for PLL-coated beads at the contact site with the neurite.

A similar experiment was also later reproduced in neonatal rat cerebellum in vivo. The study showed that PLL-coated microbeads could induce the formation of apparent presynaptic elements at 3 and 7 days (R. W. Burry et al., 1986), and 40-nm diameter synaptic vesicles were also detected at the bead contact site. Similar to the previous in vitro experiment, the number of presynaptic complexes on PLL-coated microbeads was seen to decrease at 14 and 21 days. Uncoated microbeads did not show any signs of presynaptic elements (Richard W. Burry, 1983). These experiments suggested that poly-L-lysine could promote presynaptic complex formation on microbeads both in vivo and in vitro.

.1.10 Synapse formation on microbeads in PNS studies

.1.10.1 Neuromuscular junction (NMJ)

The neuromuscular junction (NMJ) is the synaptic contact in between the terminal end of a motor nerve and a skeletal muscle (Omar et al., 2020; Slater, 2017). The main components of the NMJ include a presynaptic membrane (nerve terminals), a postsynaptic membrane (motor endplate) and a synaptic cleft. This complex structure is what allows the transmission of motor information from the CNS to the muscle fibers allowing muscle contraction. The signal transmission system found between the nerve terminals and the motor endplate is the acetylcholine neurotransmitter and its associated receptor, AChR. The acetylcholine neurotransmitter is stored in synaptic vesicles at electron-dense regions of the presynaptic membrane (active zones). Following an influx of calcium ions, the neurotransmitter is released into the synaptic cleft and binds AChRs embedded in the postsynaptic membrane leading to transient depolarization and muscle activation.

.1.10.2 In vitro studies in Xenopus larvae

Extensive research has been completed in the CNS on the use of various polybasic compounds to induce the formation of presynaptic elements onto microbeads (Richard W. Burry, 1980, 1982; Richard W. Burry, 1983; R. W. Burry et al., 1986). These studies have led to an interest in examining the effect of these basic polypeptides in the PNS. A study tested the effect of PLL-coated microbeads on motor neurons derived from Xenopus larvae embryos (H. Peng et al., 1981). The results of that study showed that PLL could induce the accumulation of acetylcholine

receptors (AChRs) clusters on microbeads when in contact with the muscle cell. However, uncoated and polycarboxylated microspheres also cultured with motor neurons did not show any clusters. Similar results were also demonstrated in another study culturing beads coated with poly-L-lysine and poly-ornithine with myotome cells (H. B. Peng et al., 1982). The study showed that postsynaptic specializations, which included AChRs clusters, membrane invaginations and basement membrane, also formed onto polybasic-coated beads at the bead-muscle contact

.1.10.3 In vivo studies in Xenopus larvae

Knowing that postsynaptic specializations could be induced on microbeads at the neuromuscular junction, the same group wanted to explore the possibility of promoting presynaptic elements on microbeads in the PNS. In a study, they investigated the effect of poly-L-lysine on latex microbeads cultured with Xenopus spinal cords (H. B. Peng et al., 1987). The results of that experiment showed that the latex beads coated with poly-L-lysine induced the formation of neuronal swellings with a high concentration of SV8, a synaptic vesicle antigen, at the bead-neurite contact. Moreover, synaptic vesicles with a diameter of 50-60 nm were observed at the contact site between the presynaptic membrane and PLL-coated microbeads. In contrast, polycarboxylated beads did not show any neuronal swellings and had lower levels of SV8 protein concentration. These findings suggested that poly-L-lysine could promote the formation of presynaptic elements on microbeads in Xenopus cultures.

.1.11 Synthetic Polymer Coatings

.1.11.1 Poly-D-Lysine (PDL)

Poly-D-Lysine is a synthetic isomer of Poly-L-Lysine (PLL). It is used as a substrate on cell cultures to promote cell adhesion and axonal outgrowth. The chemical structure of PDL is similar to PLL, but it cannot be degraded by proteases (Banket et al. 1991). The cationic charge found on the PDL molecule is what allows it to interact with the negative charge of the neuronal membrane (Kim et al., 2011). Because of these attractive properties, many studies started to investigate poly-D-lysine's ability to induce synapse formation on microbeads in the CNS. Previously, our collaborators have shown that PDL-coated microbeads cultured in hippocampal neurons can promote the formation of presynaptic boutons and synaptic vesicles at the bead-neurite contact

within 24 hours (Lucido et al., 2009). These sites were also positively-labelled with synaptophysin, bassoon and RIM as opposed to uncoated beads, which did not have any pre-synaptic boutons formed. Synaptophysin is a transmembrane protein found in presynaptic vesicles, and bassoon and RIM are scaffolding molecules in the active zone that play an important role in promoting active zone assembly, presynaptic vesicle docking and priming (Deng et al., 2011; Gundelfinger et al., 2016; Wiedenmann et al., 1985). Moreover, the presynaptic boutons observed in the study had synaptic-like function. A live cell experiment showed that these presynaptic-like endings formed onto PDL-coated microbeads could incorporate and release styryl FM-464 dye after KCl depolarization (Lucido et al., 2009). FM-464 dye is a reactive molecule used for the study of synaptic recycling (exocytosis and endocytosis) that has the capacity to enter and exit synaptic vesicles without permeating them (Iwabuchi S. et al., 2014). The observation of FM-464 dye uptake and release in the experiment suggests that these presynaptic-like structures have synaptic recycling properties similar to what is found in normal presynaptic elements. These findings were later reproduced in a cell-free in vitro system (Lucido et al., 2010). A series of experiments also demonstrated that poly-D-lysine acted through the F-actin reorganization and the heparan sulfate proteoglycans (HSPGs) transmembrane receptors, more specifically through syndecan2, to initiate the synapse formation process on microbeads (Lucido et al., 2009).

.1.11.2 Dendrimer (DND)

Dendrimer is a family of hyperbranched polyglycerols that are used as DNA carriers and drug-delivery systems (Kurniasih et al., 2015). It has the distinct structure of a core atom with radially symmetrical branches and end-groups at the periphery. The end-groups can have various functional groups altering the chemical properties of the molecule. These hyperbranched molecules are also known for their biological inertness and biocompatibility making them the ideal candidate as nanocarriers (Hellmund et al., 2014; Rajesh Kumar Kainthan et al., 2006). The stable properties of dendrimer have captured the attention of some research groups. CNS studies have shown that DND and PDL can promote the significant accumulation of synaptophysin and of vesicular acetycholine transporter (VAChT) around polystyrene microbeads when cultured onto hippocampal neurons (Al-Alwan et al. unpublished data). The VAChT protein is a transporter that mediates the loading of acetylcholine neurotransmitter into synaptic vesicles (Arvidsson U. et al.,

1997). It has been used as a reliable marker for detecting synaptic vesicles containing ACh and cholinergic neurons in the PNS and CNS.

.1.11.3 PNS studies on PDL and DND

Recent findings from our laboratory have demonstrated that the synaptogenic properties of PDL and DND found in CNS studies could translate to human IPSCs derived motor neurons. Our study showed for the first time that PDL and DND could promote significant synaptophysin and VAChT accumulation on microbeads at 1, 3, 5, 7 and 9 days in the PNS (Ma et al., 2018) (Ma et al., manuscript in preparation). The synaptophysin immunostaining was higher on microspheres for the PDL group vs. the DND group. Moreover, a live cell experiment using motor neuron cultures demonstrated that synapse-like structures formed onto DND- and PDL-coated microbeads could undergo endocytosis and exocytosis of styryl FM-143 dye following KCl depolarization. The FM-143 dye is a reactive molecule that has been used for the study of exocytosis and endocytosis (Amaral et al., 2011).

.1.12 Synaptic Marker: Synaptophysin

Various methodologies have been developed over the years to characterize synapse formation in the nervous system (Ahmari et al., 2002). They have been instrumental in the study of neurological conditions, such as schizophrenia or Alzheimer's disease (Verstraelen et al., 2018). These methods include electrophysiology, electron microscopy and immunohistochemistry (Ahmari et al., 2002). In our study, we have used an immunohistochemical approach to measure the number of presynaptic complexes formed around the microbeads in the sciatic nerve. The immunohistochemical method uses antibodies to target specific proteins located in the synaptic vesicle. One commonly targeted molecule is synaptophysin. This molecule was first discovered as a 38 kDa transmembrane protein in the cytoplasmic region of presynaptic vesicles (Jahn, 1985; Navone et al., 1986; Wiedenmann et al., 1985). It was shown to have an important role in calcium-binding (Rehm et al., 1986). Synaptophysin is also found in all nervous tissues and present in both excitatory and inhibitory terminals (Glantz et al., 2007). This synaptic protein is a reliable pan-synaptic marker that has been used in rodent and human CNS studies to measure synaptic vesicle density (Calhoun et al., 1996; Verstraelen et al., 2018). In a study examining the effect of growth-

associated protein 43 (GAP-43) on nerve growth, synaptophysin was used as a synaptic marker to track the loss and recovery of synapses in the dentate gyrus of the rat after hippocampal denervation (Masliah et al., 1991). These findings suggest that synaptophysin would be an appropriate synaptic label to use for the coated microsphere in vivo experiment.

.1.13 Research Objectives

In my master's work, I will examine the use of synthetic polymers to promote the formation of presynaptic elements onto artificial surfaces in the PNS. In the past, many innovative approaches have been used to reduce FBR in the body after the implantation of a peripheral nerve implant. These include the use of organic coatings, anti-fibrotic and immunosuppressive agents (Aregueta-Robles et al., 2014; Lotti et al., 2017). Although these methods have improved the biocompatibility of implants, FBR still occurs to a significant extent, and maintaining the long-term function of peripheral devices remains a challenge. We propose the novel strategy of using synaptogenic coatings, such as Dendrimer and Poly-D-Lysine, to reduce the effect of FBR on peripheral nerve implants. Previous studies completed by our laboratory and our collaborators have shown that DND and PDL can promote the formation of presynaptic elements onto polystyrene microbeads in vitro and in vivo (Lucido et al., 2010; Lucido et al., 2009; Ma et al., 2018). Since synapses are natural connections formed onto neurons, we believe that by promoting presynaptic elements to form onto the surface of peripheral implants, DND and PDL could help reduce the buildup of scar tissue and decrease FBR, thereby prolonging the life of the electrode. However, no prior study has demonstrated that these two synthetic polymers could have a long-lasting synapse-promoting effect on artificial surfaces in vivo. Also, no experiment has ever tested these synthetic coatings on the surface of peripheral nerve implants. Therefore, the purpose of my masters' research is to explore whether our proposed approach could be feasible using PDL and DND to promote presynaptic elements onto synthetic surfaces in the peripheral nervous system. These findings will have important future implications for the restoration of sensory feedback and motor control in patients with upper-limb amputation.

The two main research objectives of my master's are 1) to demonstrate that synthetic polymers, such as DND and PDL, can promote presynaptic elements when coated onto polystyrene

microbeads in the rat sciatic nerve model. This experiment will be a continuation of a study started by a previous master's student in our laboratory (Ma et al., 2018). Adding to that previous study, I will look at whether the synapses formed on microbeads are stable over longer periods than was previously studied. My research goals are also 2) to establish an in vivo rat model that will be used to test DND- and PDL-coated peripheral nerve implants. To accomplish this objective, I will design and develop an electrode array, establish the surgical protocol for electrode implantation and show that my implant can be used to stimulate and record nerve responses from the rat sciatic nerve.

Chapter 2 – Methods

.2 Methods

.2.1 Coated microsphere in vivo experiment

.2.1.1 Experimental design

To test the ability of DND and PDL to induce the formation of synaptic boutons on microbeads in the rat sciatic nerve, 27 male Lewis rats were used. The rats were divided into three groups: PDL, DND and CTRL condition (n = 9). For each group, three different time points were observed: 4, 6 and 8 weeks (n = 3). The sciatic nerve crush model was used in this experiment as it has been commonly used for the study of nerve repair and regeneration in the PNS (Bridge et al., 1994). The reduced cost and the anatomical similarity of the rat with human nerves make it a reliable model to study axonal regeneration (Menorca et al., 2013; Swett et al., 1986). Moreover, the Lewis rats were obtained from Charles River Laboratories, and the protocol was approved by the ethics board at CR Sainte-Justine.

.2.1.2 Bead preparation protocol

A polystyrene microbead solution (7.32 um Bangs Laboratories) containing sodium azide (100mg/mL) was used for the coated microsphere in vivo experiment. The microsphere suspension was washed and centrifuged three times with PBS before a fresh PBS solution was added. The suspension was then divided evenly between the three conditions (CTRL, DND and PDL). For the CTRL condition, the mixture was diluted with PBS solution in a 1:1 ratio. For the DND and PDL condition, a 1:9 ratio preparation of 1mg/mL DND or PDL solution and PBS was added to the microbead suspension in a 1:1 ratio. All the mixtures were then incubated overnight on a rotating device at 4°C. The mixture was then washed and centrifuged three times with PBS and added with a sterile 0.9% saline solution before used for the microinjection procedure. This technique has been used and validated for coating microbeads stably with the appropriate material (Lucido et al., 2009; Ma et al., 2018).

.2.1.3 Microinjection procedure

The surgery was performed while the rat was under isoflurane and CO_2 anesthesia. The rat was placed onto its ventral position, and an incision was performed at a 45° angle on the skin of the rat hindlimb. A narrow opening was created between the bicep femoris and gluteus maximus muscles to expose the sciatic nerve. The nerve was then completely freed from the surrounding muscles and connective tissues and was crushed using a non-serrated needle holder (Appendix Figure 4). The site was marked with India ink using a syringe needle. To investigate the regenerative process at different regions relative to the nerve injury, the DND, PDL or CTRL bead suspension (100 µL) was injected into the nerve at the crush site and 5 mm distal to the crush site using a mouth pipette (Appendix Figure 4). The wound incision on the hindlimb was then sutured back up using nylon 4-0 sutures and disinfected using 70% ethanol and Dovidine solution. Injections of 5-10 mg/kg Enrofloxacin and 0.05-0.1 mg/kg buprenorphine were administered subcutaneously to the rat on the day of the surgery and the day following the surgery.

.2.1.4 Nerve harvesting surgery

The rats were euthanized at 4, 6 and 8 weeks according to the animal facility protocol. The sciatic nerve was then exposed and cut at both ends for each rat. The nerve tissue was fixed using a 4% PFA (pH 7.0) solution for five hours with slight agitation at 4°C. The sample was then washed three times with 30% glucose solution and left in the solution for 40 hours. Afterwards, the tissue sample was dried up and embedded with OCT compound (OCT, Sakura). The embedded nerve section was then snap-frozen with dry ice and 70% ethanol before being stored in the -80°C freezer.

.2.1.5 Immunohistochemistry protocol

The OCT-embedded nerve blocks were sectioned into 14-µm thick slices at -16°C using the Leica Biosystems cryostat. The tissues were then mounted onto microscope slides (Fisherbrand Superfrost) and stored in the -80°C freezer until ready for use. When the nerve samples were ready to be stained, the slides were left at room temperature for one hour. They were then washed three times with PBS before being blocked for one hour using a solution of 0.3% Triton-X, 5% BSA and PBS. The nerve slices were then incubated overnight with primary antibodies: 1:500

rabbit anti-synaptophysin (Thermo-Fisher) and 1:500 chicken anti-neurofilament (Aves Labs 160 kDa). The slides were then washed three times with PBS before staining for two hours with secondary antibodies: 1:1000 anti-rabbit Alexa Fluor 488 (Thermo-Fisher) and 1:1000 anti-chicken Alexa Fluor 647 (Thermo-Fisher). The slides were washed three times with PBS and mounted using Fluoro-gel mounting media (Electron Microscopy Sciences) and glass coverslips. The slides were then left to dry overnight before performing any imaging. The positive control used for the experiment was rat hippocampal neuron tissues, and the negative control was rat sciatic nerve tissues without primary antibody.

.2.1.6 Confocal imaging for synaptophysin immunostaining

The image acquisition was completed using a confocal microscope (Leica TCS SP8). A 63X oil objective with a 1X magnification was used for the imaging of the newly-mounted nerve slides. The image resolution was set to 1024 X 1024 pixels, and the lasers were set to 488 nm and 633 nm corresponding to green and far-red respectively. The settings for the confocal and brightfield microscope (voltage, gain, laser power) were kept constant throughout the image acquisition process.

.2.1.7 Puncta count for in synaptophysin in vivo immunostaining

The image analysis was performed using the FIJI ImageJ Program. A minimum of 10 microbeads was analyzed for each group in the coated microsphere in vivo experiment. Microbeads stained with both synaptophysin and neurofilament were identified and selected for the analysis. In the FIJI ImageJ software, a centred circle was drawn around the circumference of the microbead using an elliptical tool in the confocal images. The confocal Z-stack image of the microbead was then examined, and the number of synaptophysin-positive puncta found in the region of the drawn circle was counted. The values were then entered into Excel 2007, and the average number of synaptophysin puncta was calculated for each group.

.2.1.8 Statistical analysis

The statistical analysis was completed using the GraphPad Prism 8 program. The synaptophysin puncta number found for the DND, PDL and CTRL groups were first compared to each other at the crush site, and then the same analysis technique was performed on these experimental

conditions at the distal site. The results of this analysis are shown in the bar graphs for the CTRL (orange), DND (purple) and PDL (blue) conditions at 4, 6 and 8 weeks (Figure 1A, B and C). An ordinary one-way ANOVA was then used with Bonferroni multi comparison test to compare the data between the experimental conditions. The sample sizes of the DND, PDL and CTRL groups satisfied the requirements for this test, and the standard error of the mean (SEM) was also included into the graphs to show the variability of the values. To further analyze the data, we plotted the average synaptophysin puncta number found for the DND, PDL and CTRL groups at 4, 6 and 8 weeks into a line graph (Figure 2A, B and C) and a histogram (Figure 3A, B and C).

.2.2 Uncoated electrode in vivo experiment

.2.2.1 Experimental design

The uncoated electrode in vivo experiment used a total of three male Lewis rats (n = 3). Two uncoated electrodes were implanted into the sciatic nerve of the rats: electrodes A and B (Appendix Figure 6). One rat did not survive the implantation surgery. The Lewis rats were obtained from Charles River Laboratories, and the protocol was approved by the animal ethics committee at CHU Sainte-Justine.

.2.2.2 Prototype electrode fabrication

The uncoated electrode design was composed of a headstage connector (Omnetics Connector Corporation) and four wires: recording (green), stimulation (yellow), ground (white) and reference (brown) (Appendix Figure 6). The headstage connector served as a connection between the wires and the headstage (or signal transmitting system) (Appendix Figure 7B). The recording and reference wires were fabricated by removing a 1-mm section of wire insulation from a Pt-Ir microwire (Worlds Precision Instruments 50 AWG) using a surgical scalpel. The tip of the recording microwire was soldered to a needle allowing for threading and placement of the wire into the sciatic nerve. For the stimulation and ground electrodes, two microwires (Conner wires) were glued together using Epoxy paste and bent into the shape of a hook. The hook structure was to ensure that the electrodes were securely attached to the sciatic nerve during the implantation surgery and nerve recordings.

.2.2.3 Electrode implantation surgery

The surgery was performed while the rat was under isoflurane and CO_2 anesthesia. The rat was placed onto its ventral position, and an incision was performed at a 45° angle on the skin of the rat hindlimb. The sciatic nerve was exposed using a similar procedure to the microinjection surgery (see .2.1.3 Microinjection procedure). The reference, stimulation, ground and recording wires were then implanted individually into the rat sciatic nerve. The recording wire was carefully threaded into the sciatic nerve until the 1-mm exposed end of the microwire was completely within the nerve fascicle. The stimulation and ground electrodes were hooked around the nerve to keep the implant into position, and the reference wire was placed subcutaneously. Slight adjustments were made to the wire placement before the leg incision was sutured back up using nylon 4-0 sutures. The wound opening was then disinfected using 70% ethanol and Dovidine solution after the surgery.

After the wires were implanted into the sciatic nerve, an incision was performed on the rat head to expose the cranium. The surrounding skin and connective tissues were removed using a surgical scalpel. Two holes were created into the skull on top of the somatosensory cortex using a mechanical drill and were used to attach the headstage later on. The uncoated electrodes implanted into the rat sciatic nerve were then entirely coated with Polysporin antibiotic ointment. The headstage connector and the wires were then carefully passed subcutaneously in the dorsal part of the rat from the leg incision to the head incision using a knitting needle. The headstage connector of the electrode was then securely fixed to the skull using dental cement in addition to the metal screws. Injections of 5-10 mg/kg of Enrofloxacin and 0.05-0.1 mg/kg of buprenorphine were then administered to the rat on the day of the surgery and the day following the surgery.

.2.2.4 Nerve stimulation and recording protocol

A wireless data acquisition system (Multichannel W2100 System) was used to perform the electrical stimulations and nerve recordings for the uncoated electrodes in the rat sciatic nerve (Appendix Figure 7A). This system was chosen for the experiment because the headstage could fit on the head of the rat and could transmit information wirelessly to the acquisition system (Appendix Figure 7B). The nerve recordings were performed on the day of the implantation and on every week using the electrodes A and B, and they were conducted while the rat was under

isoflurane and CO_2 anesthesia. Electrical stimulations were used for the uncoated electrode in vivo experiment because the rat was under anesthesia. The anesthetized state of the rat inhibited the neural activity detected in the sciatic nerve requiring external stimulation for the observation of nerve signals in the recordings.

After completing the electrode implantation surgery, we calibrated the headstage with the acquisition system and tested our electrode set-up on the day of the implantation. Stimulations with a pulse duration of 600 µs and amplitude of 150, 160 and 170 µA were performed on the sciatic nerve (Appendix Figure 10). The uncoated electrodes were then kept into the rat and weekly recordings were performed in the rat sciatic nerve using the implants. The pulse amplitude used for the weekly sessions was a 250 µA biphasic square-wave pulse. During the data acquisition process, we also applied a high-pass notch filter with a cut-off frequency of 0.1 Hz to remove the background noise. To monitor the long-term signal stability of the implant, we measured the minimum pulse duration required to trigger threshold nerve potential in the rat sciatic nerve every week. To measure this value, we set the pulse duration of the stimulation to an arbitrary value and increased it by 10 µs increments until a muscle twitch was observed. We then decreased the pulse duration until the threshold nerve potential was detected in the nerve recordings. The muscle contraction and EMG recordings in the rat hindlimb were also used as a visual cue to determine whether the nerve stimulation was successful or not. The protocol used was similar to the one applied in an experiment that tested the long-term function of Utah slanted electrode arrays in cat sciatic nerve (Branner et al., 2004). The in vivo data was then processed using the Multichannel W2100 System software to filter out the background noise from the nerve signals. The data points for the two implants were then plotted into PowerPoint 2007. The minimum pulse duration required to trigger a nerve response in the rat sciatic nerve for both electrodes A and B was plotted against the number of weeks post-implantation.

.2.2.5 Nerve harvesting surgery

After electrode failure of both uncoated electrodes, the rats were euthanized according to the animal facility protocol. The rat leg incision was reopened, and the sciatic nerve was exposed using a similar procedure to the electrode implantation surgery (see .2.2.3 Electrode implantation surgery). The electrode wires were carefully extracted from the sciatic nerve (Appendix Figure

8B), and the nerve and electrode were examined macroscopically for signs of scar tissue formation and physical wear of the electrode itself.

Chapter 3 – Results

.3 Results

.3.1 Coated microsphere in vivo experiment

.3.1.1 DND and PDL induced significant synaptophysin accumulation on microspheres in vivo for both the crush and distal sites, at weeks 4, 6 and 8 weeks post-injection when compared to CTRL

In the coated microsphere in vivo experiment, a nerve crush injury was made in the rat sciatic nerve and PDL-coated, DND-coated and uncoated microbeads were then injected at two nerve sites: the crush site and 5 mm distal to the crush site (Figure 1). The sciatic nerves were harvested at 4, 6 and 8 weeks post-injection and stained with synaptophysin and neurofilament antibodies. Confocal images were then taken of PDL-coated, DND-coated and uncoated microbeads that were injected into the sciatic nerve. The results of this study showed that many synaptophysin-positive puncta formed on the surface of microbeads in the PDL and DND group after 4, 6 and 8 weeks. An example of these synaptophysin puncta could be observed as synaptic vesicles positively-labelled with synaptophysin (green) on the surface of microbeads in confocal images (Figure 2). To quantify the synaptophysin accumulation on the microbeads, I counted the number of synaptophysin puncta found on each microbead surface and calculated the average number for PDL-coated, DND-coated and uncoated beads. The average synaptophysin puncta number was calculated by adding the raw values obtained for all three rats in a group and dividing it by the total number of microbeads analyzed for the condition (n). This study showed for the first time that the DND-coated microbeads could promote a higher synaptophysin accumulation on their surface compared to CTRL beads at 4 and 6 weeks for the crush site in vivo (Bonferroni's post hoc test, $n_{CTRL} = 37$ and $n_{DND} = 70$, $p = 0.0188$, for 4 weeks, and $n_{CTRL} = 66$ and $n_{DND} = 102$, $p = 0.0005$, for 6 weeks) (Figure 3A and B). As for the distal site, the DND group had a superior synaptophysin accumulation on its microbeads at 4, 6 and 8 weeks compared to the CTRL group (Bonferroni's post hoc test, $n_{CTRL} = 41$ and $n_{DND} = 85$, $p = 0.0095$, for 4 weeks, $n_{CTRL} = 105$ and $n_{DND} = 89$, $p < 0.0001$, for 6 weeks, and $n_{CTRL} = 55$ and $n_{DND} = 24$, $p = 0.0441$, for 8 weeks) (Figure 3A, B

and C). In this experiment, I also observed that at 6 weeks, the PDL-coated microbeads induced a higher synaptophysin accumulation compared to the CTRL microbeads for the distal site (Bonferroni's post hoc test, n_{CTRL} = 105 and n_{PDL} = 46, p = 0.0256) (Figure 3B), despite being nonsignificant for the other tested time points and nerve sites (Bonferroni's post hoc test, p > 0.05) (Figure 3A, B and C). When DND and PDL were compared, the results also showed that at 4 weeks, the DND-coated microspheres promoted a higher synaptophysin accumulation on their surface compared to PDL-coated microbeads for the distal site (Bonferroni's post hoc test, n_{DND} = 85 and n_{PDL} = 62, p = 0.0043) (Figure 3A). From these observations, DND seems to promote better synaptophysin accumulation on microbeads compared to CTRL from 4 to 8 weeks and compared to PDL at 4 weeks in vivo. As for PDL, it can promote better synaptophysin accumulation compared to CTRL at 6 weeks.

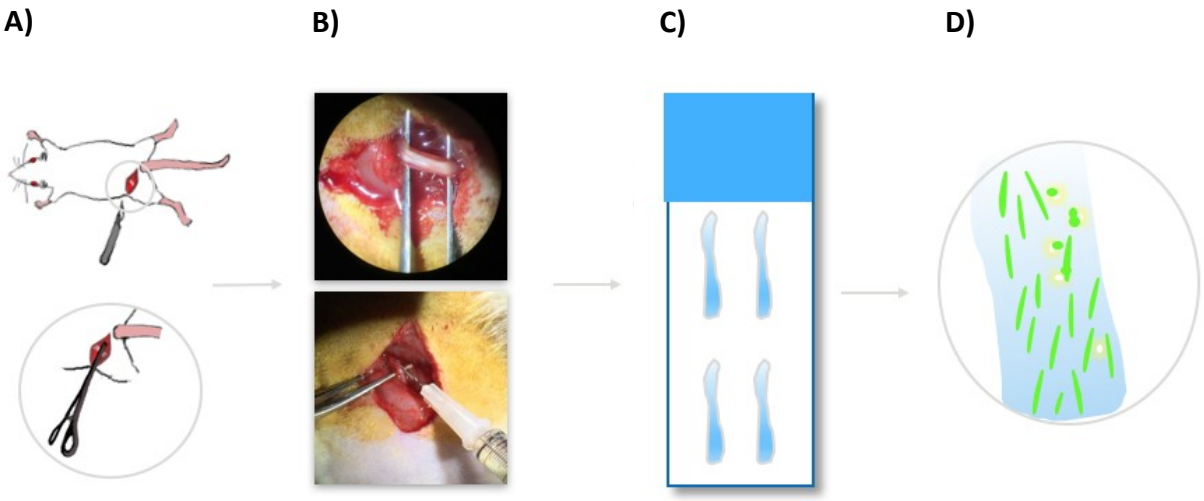

Figure 1. – Representative image of the experimental design for the coated microsphere in vivo experiment at 4, 6 and 8 weeks for the CTRL, DND and PDL groups: A) The nerve crush procedure where the rat sciatic nerve was exposed and crushed using a non-serrated needle holder B) The microinjection procedure where PDL-, DND-coated and uncoated microbead solutions were injected into the rat sciatic nerve using a mouth pipette C) A 14-µm thick rat sciatic nerve tissue on a glass slide stained with 1:500 rabbit synaptophysin (Thermo-Fisher) and 1:500 chicken neurofilament antibodies (Aves Labs 160 kDa) D) The confocal images of a

rat sciatic nerve tissue slide acquired using a 63X oil objective at 1X magnification with lasers at 488 nm and 633 nm. Reproduction with permission from Dr. Jenny Lin's laboratory.

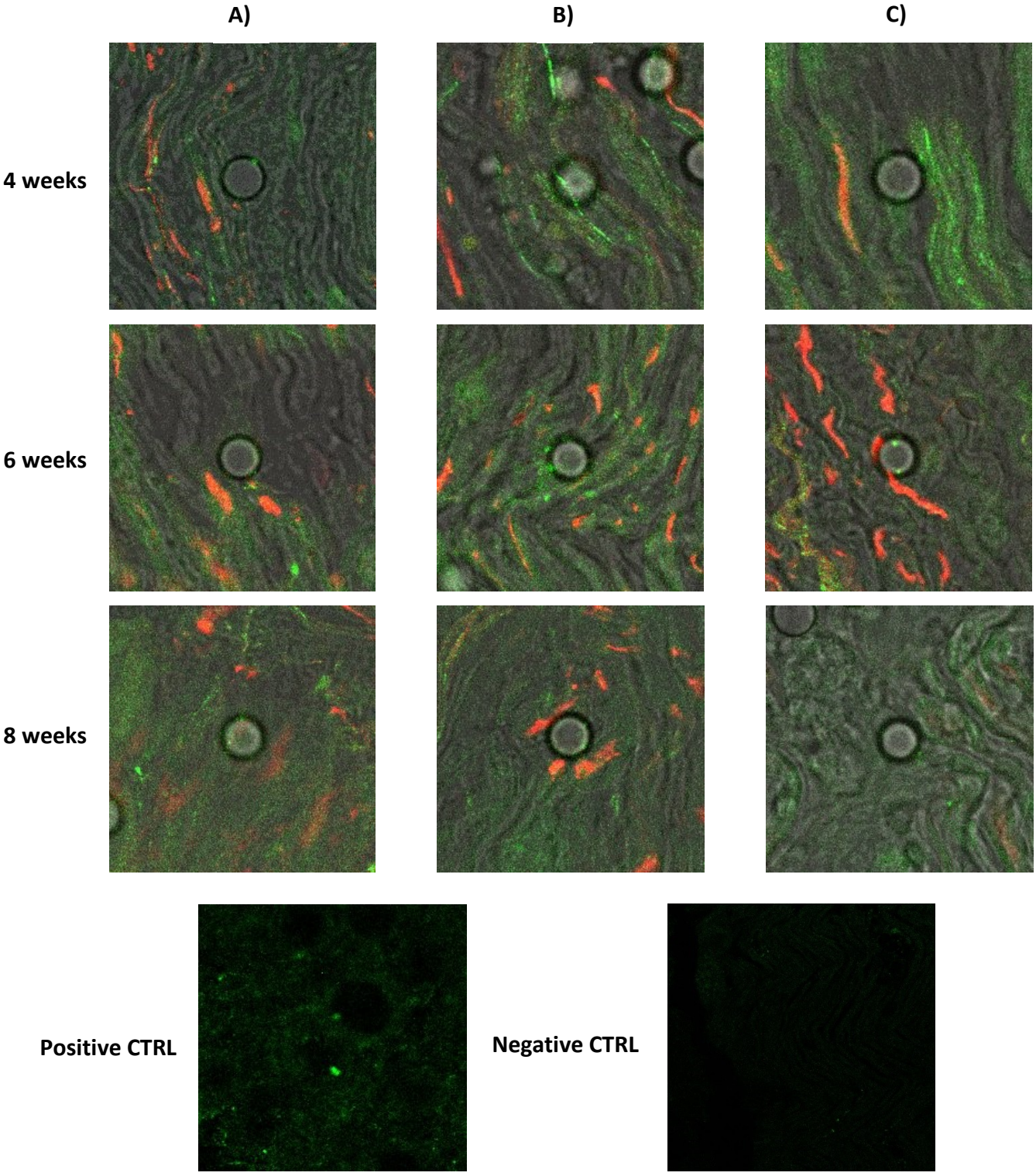

Figure 2. – Series of images taken using a confocal and brightfield microscope of the microbeads injected into 14 µm thin sections of rat sciatic nerve stained with synaptophysin (green) and neurofilament (red) at 4, 6 and 8 weeks for the experimental conditions : A) CTRL, B) DND and C) PDL. Positive CTRL: rat hippocampal neuron tissues; Negative CTRL: rat sciatic nerve tissues without primary antibody.

A)

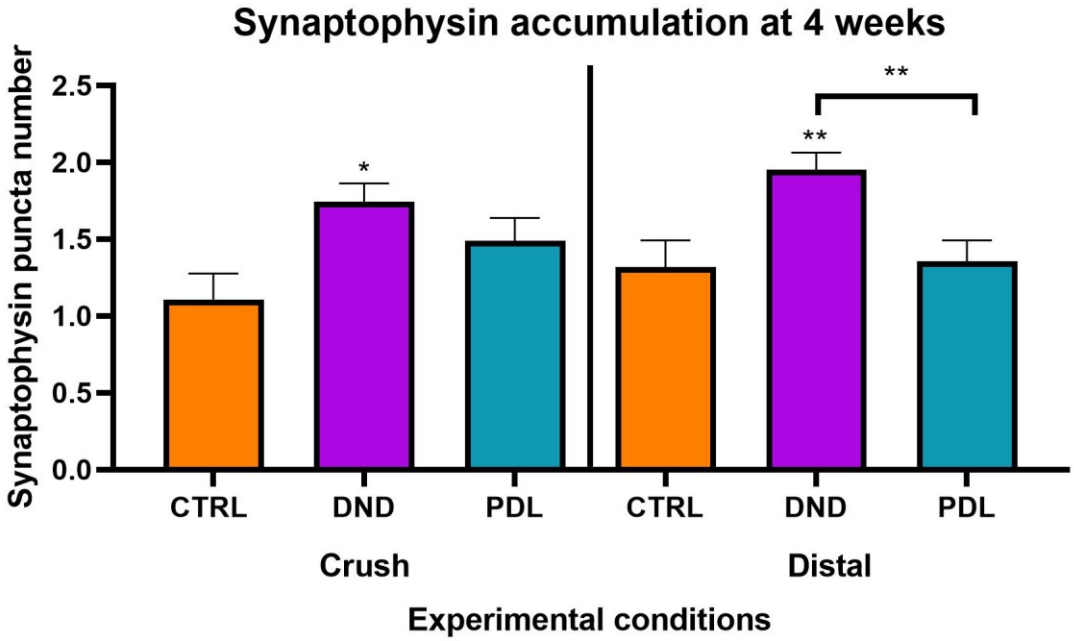

B)

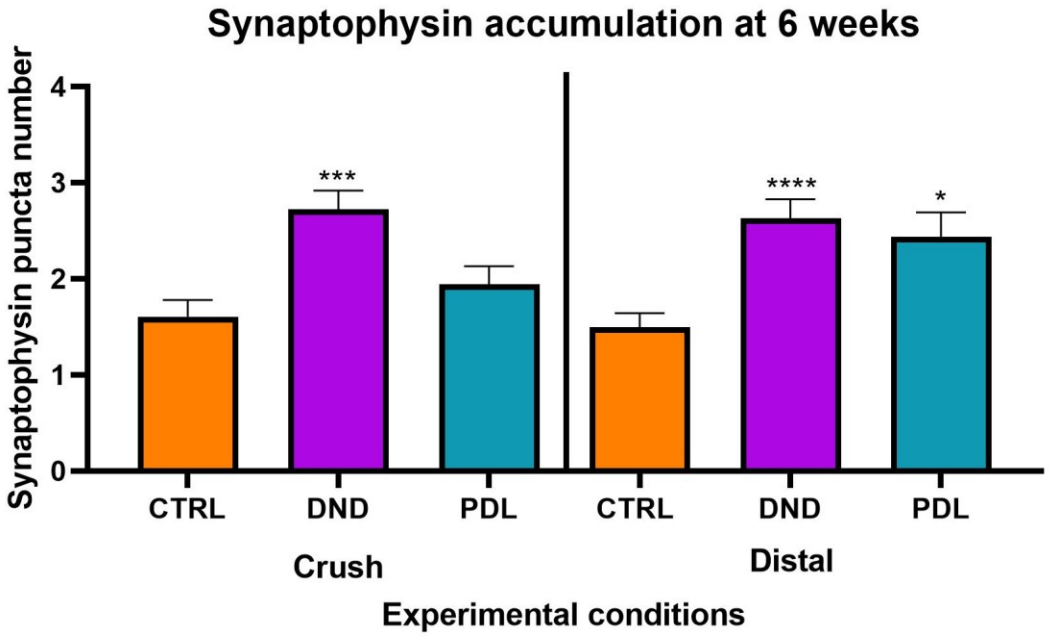

C)

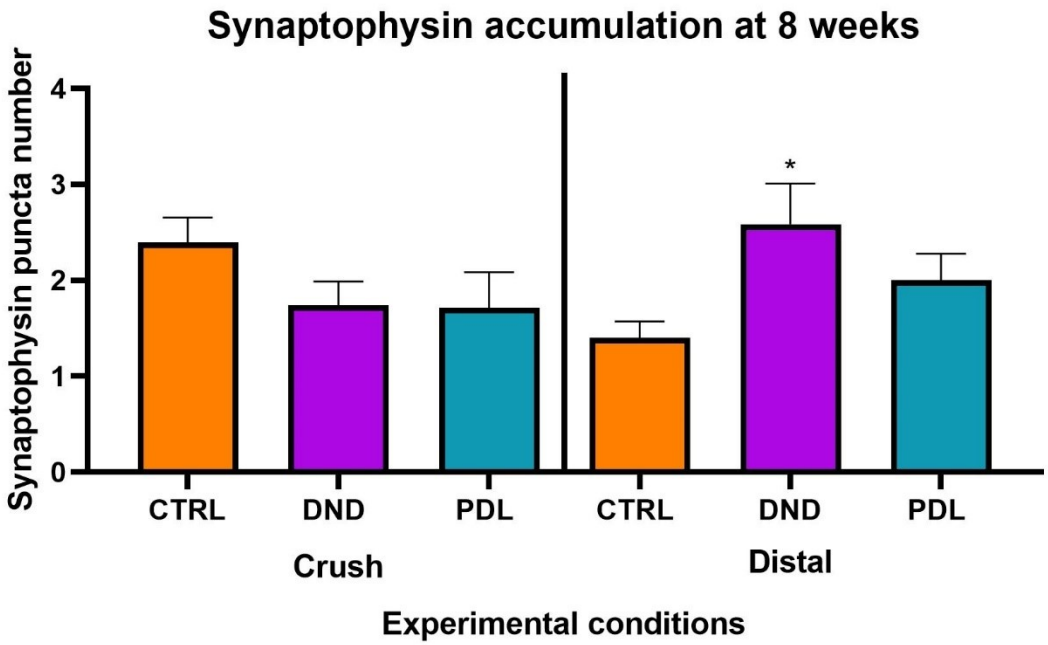

Figure 3. – The average number of puncta with synaptophysin immunostaining per microbead in the CTRL, DND and PDL groups in the rat sciatic nerve for the crush and distal sites at 4, 6 and 8 weeks.

The average number of puncta per microbead for each group was obtained through adding the raw synaptophysin puncta number values measured for the microbeads of all three rats in a condition and dividing it by the total number of microbeads analyzed for the group (n): A) 4 weeks for the crush (CTRL n = 37, DND n = 70, PDL n = 51) and distal sites (CTRL n = 41, DND n = 62, PDL n = 85) B) 6 weeks for the crush (CTRL n = 66, DND n = 102, PDL n = 50) and distal sites (CTRL n = 105, DND n = 89, PDL n = 46) C) 8 weeks for the crush (CTRL n = 53, DND n = 14, PDL n = 19) and distal sites (CTRL n = 55, DND n = 24, PDL n = 32). One-way ANOVA (Average ± SEM), * $p \leq 0.05$, ** $p \leq 0.01$, *** $p \leq 0.001$, **** $p \leq 0.0001$.

.3.1.2 Synaptophysin puncta number on microbeads over time in the CTRL, DND and PDL groups in vivo

After acquiring the data at all these time points, we were interested in looking at how the synaptophysin accumulation on the surface of microbeads would change over time for the CTRL, DND and PDL groups at both the crush and distal sites. This analysis was important for knowing

whether the newly-formed synaptophysin puncta on the coated microbeads were stable between 4 to 8 weeks. Using GraphPad Prism 8, I plotted into a line chart the average synaptophysin puncta number found for each condition in Figure 3. over the tested time points of the experiment (4, 6 and 8 weeks). When looking at the crush site, the results showed that the DND-coated microbeads had a stable synaptophysin puncta number on their surface at 4 and 6 weeks (Bonferroni's post hoc test, n_{CTRL} = 37 and n_{DND} = 70, p = 0.0188, at 4 weeks and n_{CTRL} = 66 and n_{DND} = 102, p = 0.0005, at 6 weeks) before decreasing to baseline values at 8 weeks (Bonferroni's post hoc test, n_{CTRL} = 53 and n_{DND} = 19, p > 0.9999) (Figure 4A). As for the PDL group, the synaptophysin accumulation values were similar to the ones found for the CTRL group at the crush site (Figure 4A). The number of synaptophysin puncta obtained for the PDL-coated microbeads was close to baseline values at 4, 6 and 8 weeks (Bonferroni's post hoc test, n_{CTRL} = 37 and n_{PDL} = 51, p = 0.5566, for 4 weeks, and n_{CTRL} = 66 and n_{PDL} = 50, p > 0.9999 for 6 weeks, and n_{CTRL} = 53 and n_{PDL} = 14, p > 0.9999, for 8 weeks) (Figure 4A). When comparing the different conditions, we also found that DND had a higher average synaptophysin puncta number compared to PDL at 4 weeks (Bonferroni's post hoc test, n_{CTRL} = 85 and n_{PDL} = 62, p = 0.0043).

Similar results were also found for the DND and PDL groups when looking at the distal site. Our results showed that the DND group had increased accumulation of synaptophysin puncta on its microbeads at 4, 6 and 8 weeks (Bonferroni's post hoc test, n_{CTRL} = 41 and n_{DND} = 85, p = 0.0095, for 4 weeks, n_{CTRL} = 105 and n_{DND} = 89, p < 0.0001, for 6 weeks, and n_{CTRL} = 55 and n_{DND} = 24, p = 0.0441, for 8 weeks) (Figure 4B). As for the PDL group, the synaptophysin puncta number started at baseline values at 4 weeks for the distal site (Bonferroni's post hoc test, n_{CTRL} = 37 and n_{DND} = 51, p > 0.9999) (Figure 4B). The number of synaptophysin puncta then increased at 6 weeks (Bonferroni's post hoc test, n_{CTRL} = 105 and n_{DND} = 46, p = 0.0256) before returning to baseline values at 8 weeks (Bonferroni's post hoc test, n_{CTRL} = 55 and n_{DND} = 32, p > 0.9999). When comparing the experimental groups, we also observed that the synaptophysin accumulation values were higher for the DND group compared to the PDL group, despite being non-significant at 4, 6 and 8 weeks (Bonferroni's post hoc test, n_{CTRL} = 37 and n_{DND} = 51, p > 0.9999, for 4 weeks, n_{CTRL} = 89 and n_{DND} = 46, p > 0.9999, for 6 weeks, and n_{CTRL} = 24 and n_{DND} = 32, p > 0.9999, for 8 weeks). From these observations, the DND-coated microbeads seem to have a stable

synaptophysin accumulation on its surface from 4 to 6 weeks for the crush site and from 4 to 8 weeks for the distal site in vivo.

A)

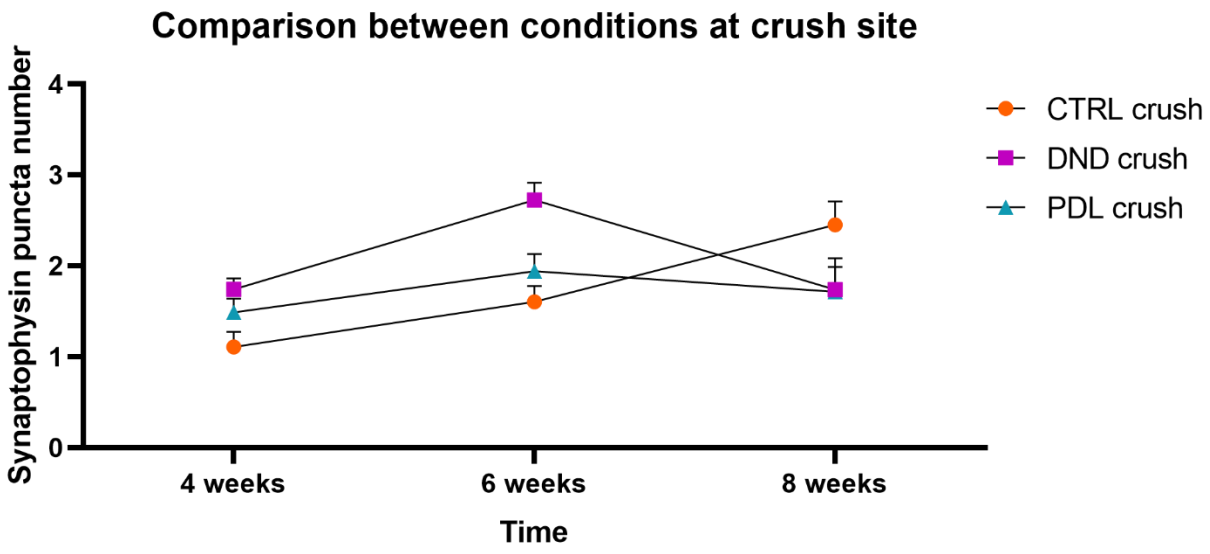

B)

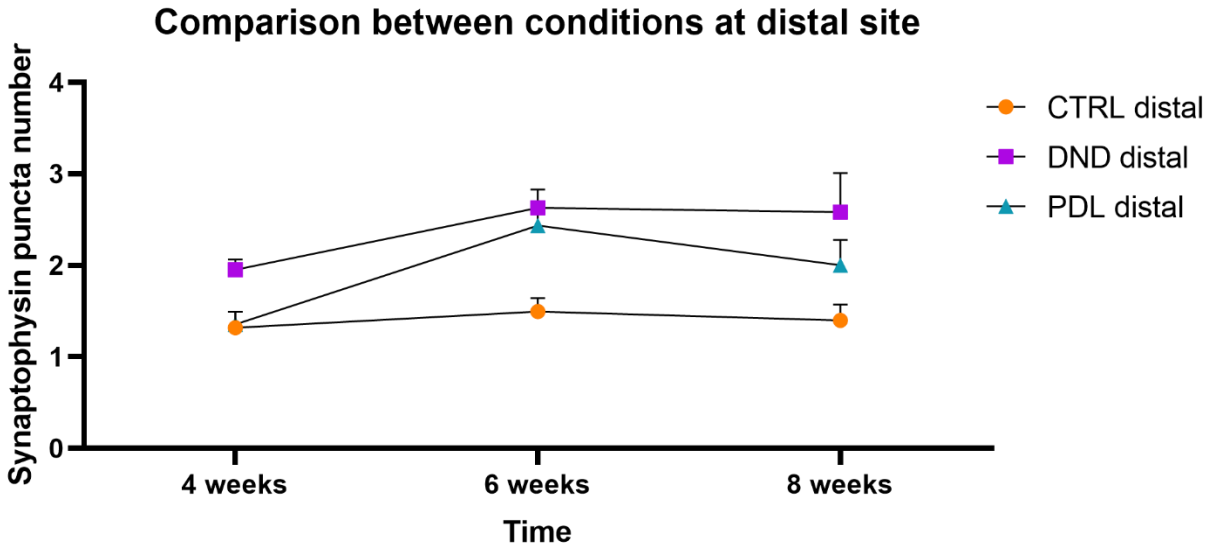

Figure 4. – The change in the average number of synaptophysin puncta found on the surface of microbeads in the CTRL, DND and PDL groups at 4, 6 and 8 weeks.

The line graph was obtained through plotting the average synaptophysin puncta number calculated for each group in Figure 3. over the tested time points of the study (4, 6 and 8 weeks), where n is the total number of microbeads analyzed for all three rats in a condition:

A) crush site (4 weeks: CTRL n = 37, DND n = 70, PDL n = 51, 6 weeks: CTRL n = 66, DND n = 102, PDL n = 50, and 8 weeks: CTRL n = 53, DND n = 14, PDL n = 19) B) distal site (4 weeks: CTRL n = 41, DND n = 62, PDL n = 85, 6 weeks: CTRL n = 66, DND n = 102, PDL n = 50, and 8 weeks: CTRL n = 55, DND n = 24, PDL n = 32). One-way ANOVA (Average ± SEM). * $p \leq 0.05$, ** $p \leq 0.01$, *** $p \leq 0.001$, **** $p \leq 0.0001$.

.3.1.3 Bead distribution for the DND, PDL and CTRL groups at 4, 6 and 8 weeks

After looking at the change of synaptophysin accumulation over time, I then examined the bead distributions for the DND-coated, PDL-coated and uncoated microbeads at 4, 6 and 8 weeks. Using GraphPad Prism 8, I plotted into a histogram the raw synaptophysin puncta values used to calculate the average for each group in Figure 3. The values grouped either as 0, 1 or 2 or more synaptophysin puncta per bead were represented as a bead frequency. These results showed that at 4 weeks, a higher frequency of DND-coated microbeads had two or more synaptophysin puncta on their surface compared to CTRL microbeads for both the distal (X^2 (2, N = 107) = 8.812, p = 0.0122) and crush sites (X^2 (2, N = 126) = 8.631 p = 0.0134) (Figure 5A). This is represented in the bar graph as the purple (DND group) and orange (CTRL group) frequency distributions (Figure 5A). Similar results were also observed at 6 weeks between the DND and the CTRL conditions for both the crush (X^2 (2, N = 168) = 10.58, p = 0.005) and distal sites (X^2 (2, N = 194) = 16.05, p = 0.0003) (Figure 5B). However, the bead distribution did not differ significantly between the two groups at 8 weeks for the crush (X^2 (2, N = 79) = 2.643, p = 0.2267) and distal sites (X^2 (2, N = 72) = 0.03673, p = 0.9818) (Figure 5C).

When looking at the PDL group, our results showed that the bead distribution at 4 weeks did not differ significantly from the CTRL group for both the crush (X^2 (2, N = 88) = 2.828, p = 0.2432) and distal sites (X^2 (2, N = 103) = 0.1586, p = 0.9238) (Figure 5A). This could be seen in the bar graph as the blue (PDL condition) and orange (CTRL condition) frequency distributions (Figure 5A). Similar results were found between the two conditions at 6 weeks (X^2 (2, N = 116) = 2.273, p = 0.3209 for the crush site) and 8 weeks (X^2 (2, N = 69) = 0.5469, p = 0.7608 for the crush site, and X^2 (2, N = 87) = 1.663, p = 0.4354 for the distal site) (Figure 5B and C). The bead distribution only differed significantly between PDL and CTRL at 6 weeks for the distal site (X^2 (2, N = 151) = 7.613, p = 0.0222) (Figure 5B). From these observations, only the DND condition seems to have a bead

distribution that has a significantly higher frequency of microbeads with two synaptophysin puncta or more compared to the CTRL condition at 4 and 6 weeks in vivo.

A)

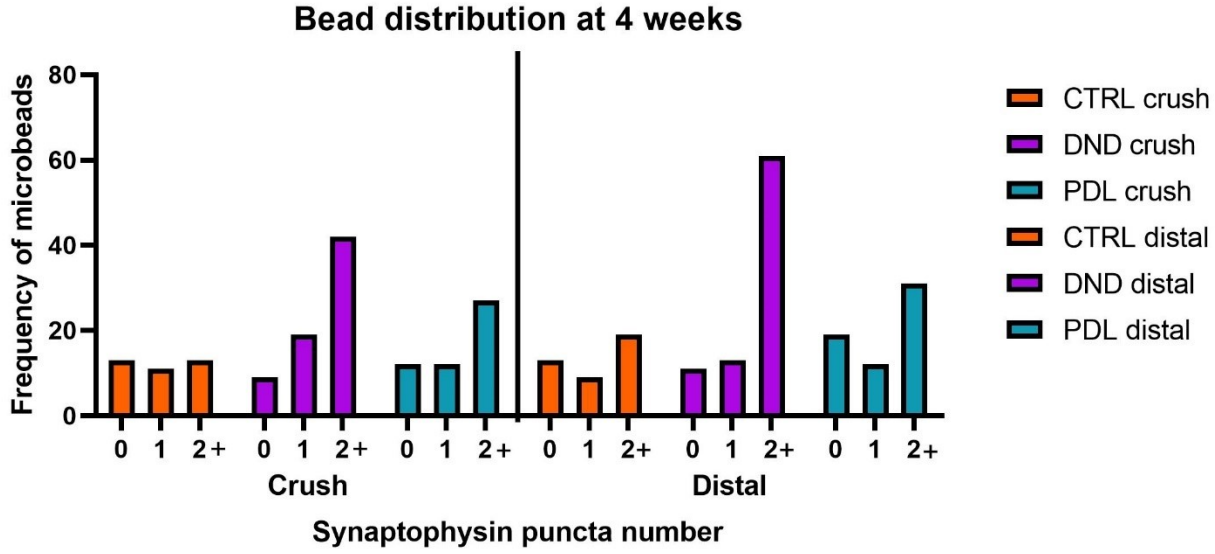

B)

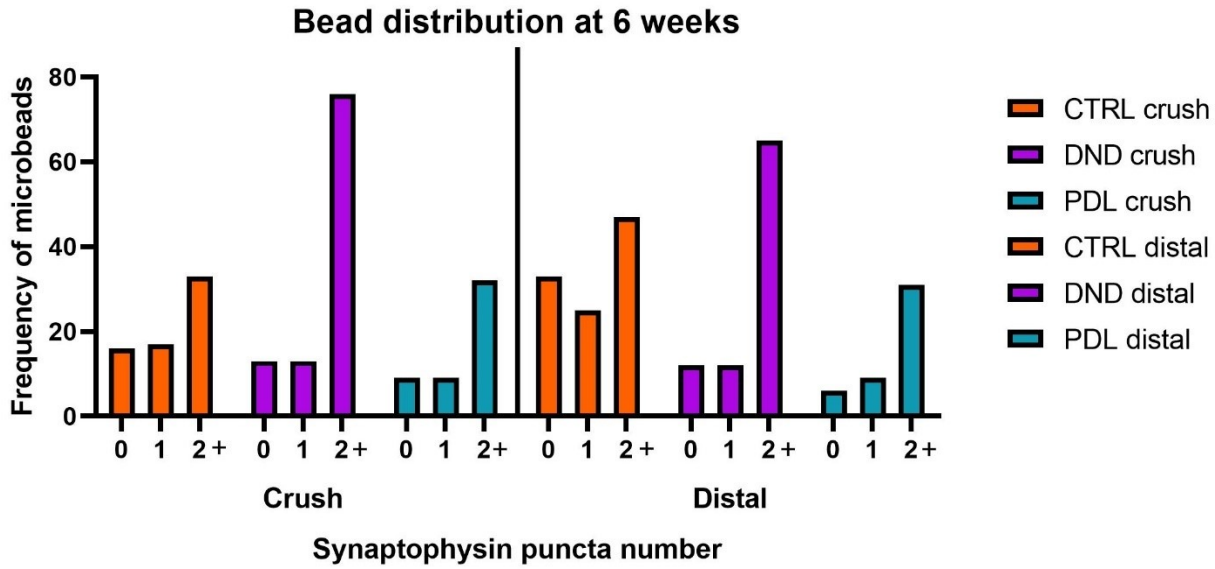

C)

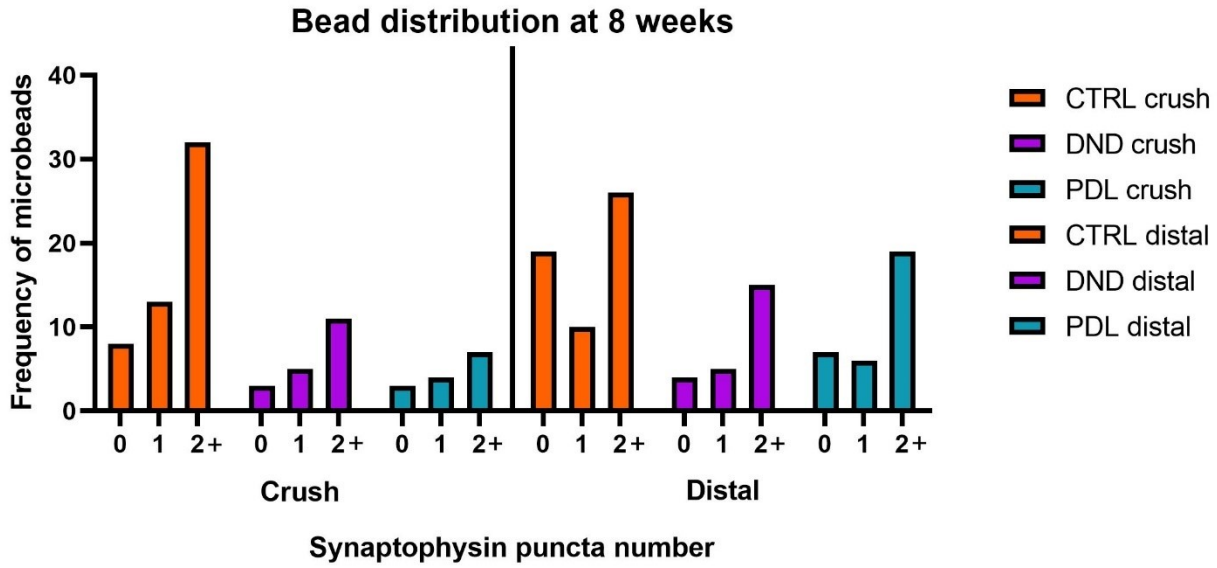

Figure 5. – Bead distributions for the frequency of microbeads with 0, 1 and 2 or more synaptophysin puncta number on their surface in the experimental conditions (CTRL, DND and PDL) for the crush and distal sites at the 4, 6 and 8 weeks.

The frequency of microbeads found for each condition was obtained by binning the raw synaptophysin puncta values measured for the microbeads of all three rats in a group into either 0, 1 or 2 or more synaptophysin puncta per bead: A) 4 weeks for the crush (CTRL n = 37, DND n = 70, PDL n = 51) and distal sites (CTRL n = 41, DND n = 62, PDL n = 85) B) 6 weeks for the crush (CTRL n = 66, DND n = 102, PDL n = 50) and distal sites (CTRL n = 105, DND n = 89, PDL n = 46) C) 8 weeks for the crush (CTRL n = 53, DND n = 14, PDL n = 19) and distal sites (CTRL n = 55, DND n = 24, PDL n = 32). Then, I performed multiple chi-square tests between the DND or PDL group vs. the CTRL group for 4, 6 and 8 weeks with an $\alpha = 0.05$ using the frequency of microbeads with 0, 1 and 2 or more synaptophysin puncta. The null hypothesis used for the chi-square tests was that the bead distribution for the DND or PDL group followed what is found in the CTRL group. The alternative hypothesis was that the distribution of microbead frequency for the DND or PDL group differed from what is found in the CTRL group.

.3.2 Uncoated electrode in vivo experiment

.3.2.1 Uncoated electrodes stimulated and recorded threshold nerve potentials from the rat sciatic nerve in vivo

In the uncoated electrode in vivo experiment, two thin-wire Pt-Ir uncoated electrodes (A and B) were implanted into the sciatic nerve of Lewis rats (n = 2) (Appendix Figure 9). The recording, stimulation and ground wires of the uncoated electrodes were implanted into the sciatic nerve, and the reference wire was left subcutaneously in the rat. The headstage of the implant was anchored to the rat skull using dental cement and metal screws (Appendix Figure 10B). For our electrode set-up, a Multichannel W2100 System was used to communicate wirelessly with the headstage found on the rat head (Appendix Figure 10A). This system allowed us to send electrical stimulation to the sciatic nerve of the rat through the stimulation wire of our uncoated electrode and to acquire nerve responses through the recording wire. After completing the implantation procedure, we tested our system by performing electrophysiological recordings on the rat. Our results demonstrated that the system could stimulate and record nerve potentials from the rat sciatic nerve at varying pulse amplitudes and durations on the day of the implantation (t = 0). This could be seen in the nerve recordings as a stimulation wave at t = 0 ms marked by the blue arrow triggering a nerve potential at t = 2 ms marked by the red circle (Figure 6A). After the nerve stimulation, a muscle twitch was also observed at the level of the rat leg. This procedure was then repeated with stimulations at pulse amplitudes of 160 and 170 µA (Figure 6B and C).

After showing that the electrode set-up could trigger and record nerve potentials, we kept the implant in the rat sciatic nerve and recorded nerve responses every week until the electrode failed. A pulse amplitude of 250 µA was used for the stimulation throughout the recordings. We then measured the minimum pulse duration required to trigger a threshold nerve potential in the rat sciatic nerve every week. Our study showed that the pulse duration required to trigger a threshold nerve potential increased from 320 µs to 1000 µs for electrode A in the first week after the implantation (Figure 7B). In the second week of recording, the pulse duration increased to 1200 µs (Figure 7C). This process continued until the implant stopped functioning in week 3. This was shown in the nerve recordings at week 3 by the missing threshold nerve potential after the

pulse stimulation at t = 0 ms marked by the blue arrow (Figure 7D). We also did not detect any muscle twitch from the rat leg after applying an electrical stimulation. The electrode B had a similar outcome to the electrode A. In the first week of testing, the electrode B needed to increase the pulse duration of the stimulation from 400 µs to 1000 µs to trigger a threshold nerve potential (Figure 8B). At week 2, the implant could no longer acquire any nerve response from the rat sciatic nerve or any EMG signal from the muscle. The decreased signal stability of electrodes A and B was also represented using a line graph with the minimum pulse duration required to trigger a threshold nerve potential plotted over time for both implants (Appendix Figure 9). This data demonstrates progressive loss of ability of the electrode to stimulate and record over time.

A)

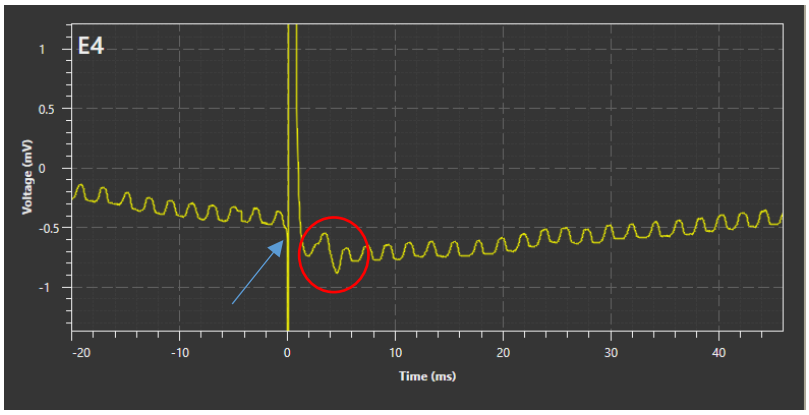

B)

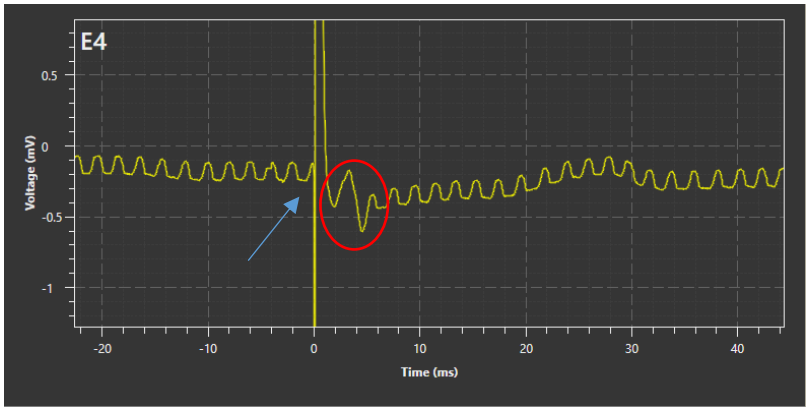

C)

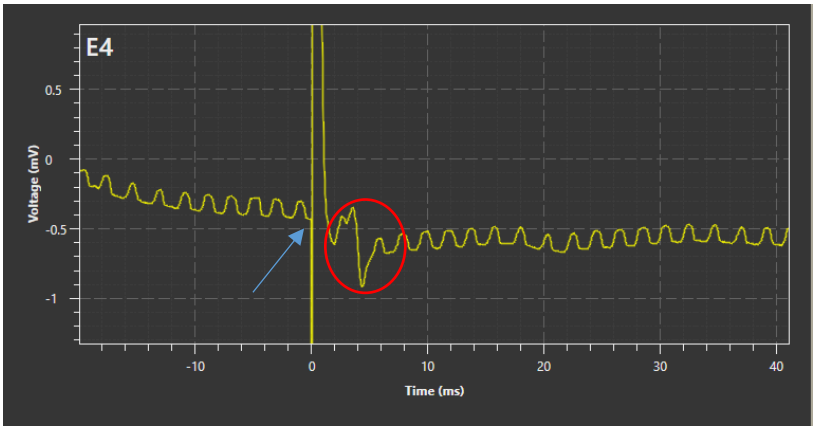

Figure 6. – Electrophysiological recordings for electrode A on the day of the implantation (t = 0) at 600 µs at varying pulse amplitudes of: A) 150 µA B) 160 µA C) 170 µA. Blue arrow: biphasic square-wave stimulation pulse at (t = 0 ms); Red circle: threshold nerve potential.

A)

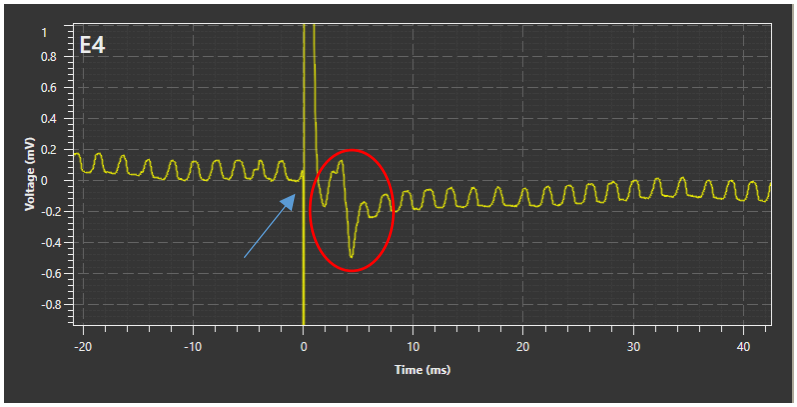

B)

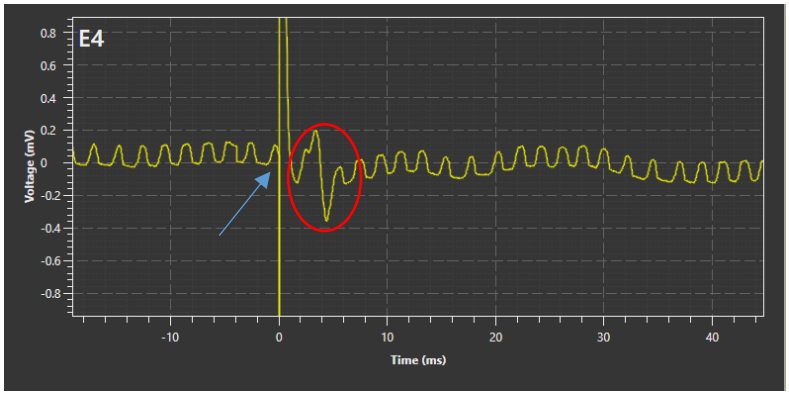

C)

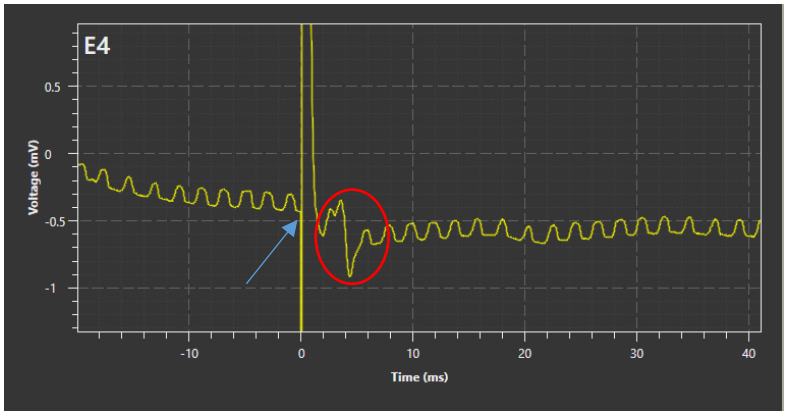

D)

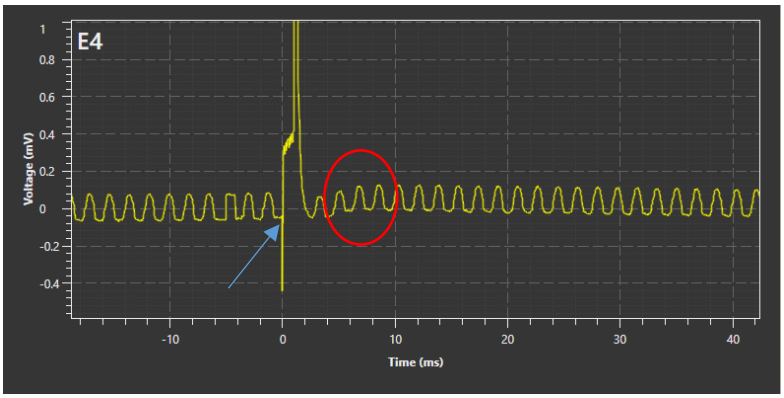

Figure 7. – Electrophysiological recordings at 250 µA for electrode A on: A) the day of the implantation (t = 0) B) week 1 C) week 2 D) week 3. Blue arrow: biphasic square-wave stimulation pulse at (t = 0 ms); Red circle: threshold nerve potential.

A)

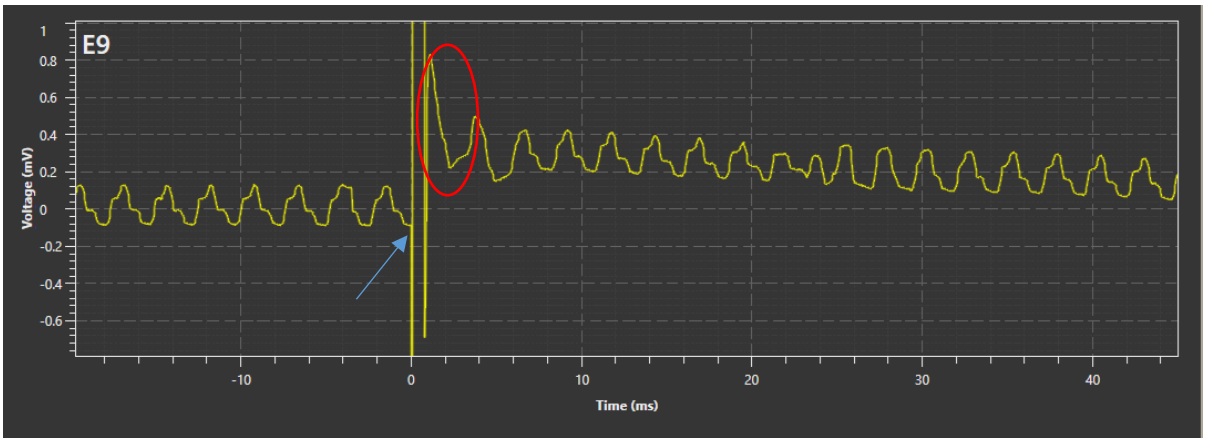

B)

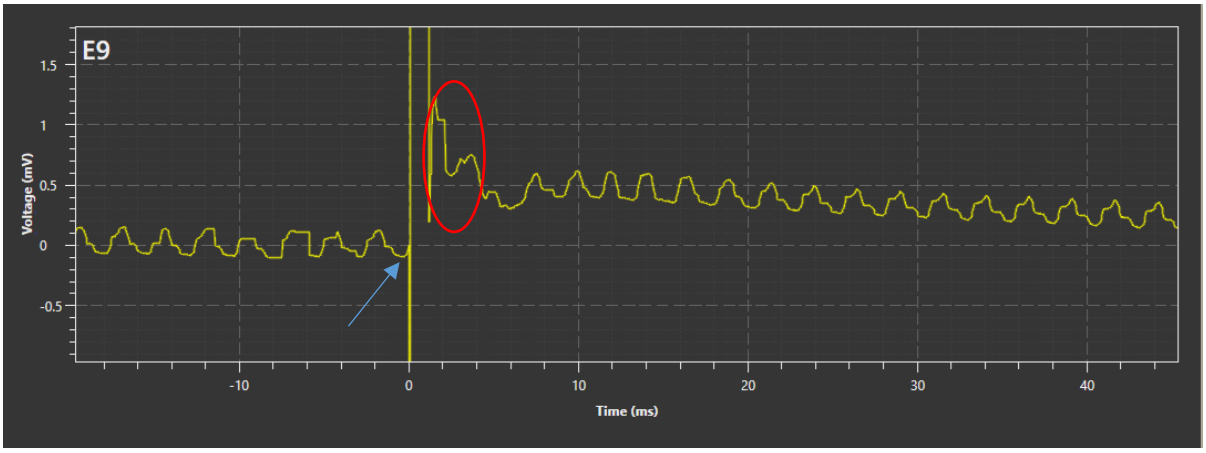

Figure 8. – Electrophysiological recordings at 250 µA for electrode B on: A) the day of the implantation (t = 0) B) week 1. Blue arrow: biphasic square-wave stimulation pulse at (t = 0 ms); red circle: threshold nerve potential.

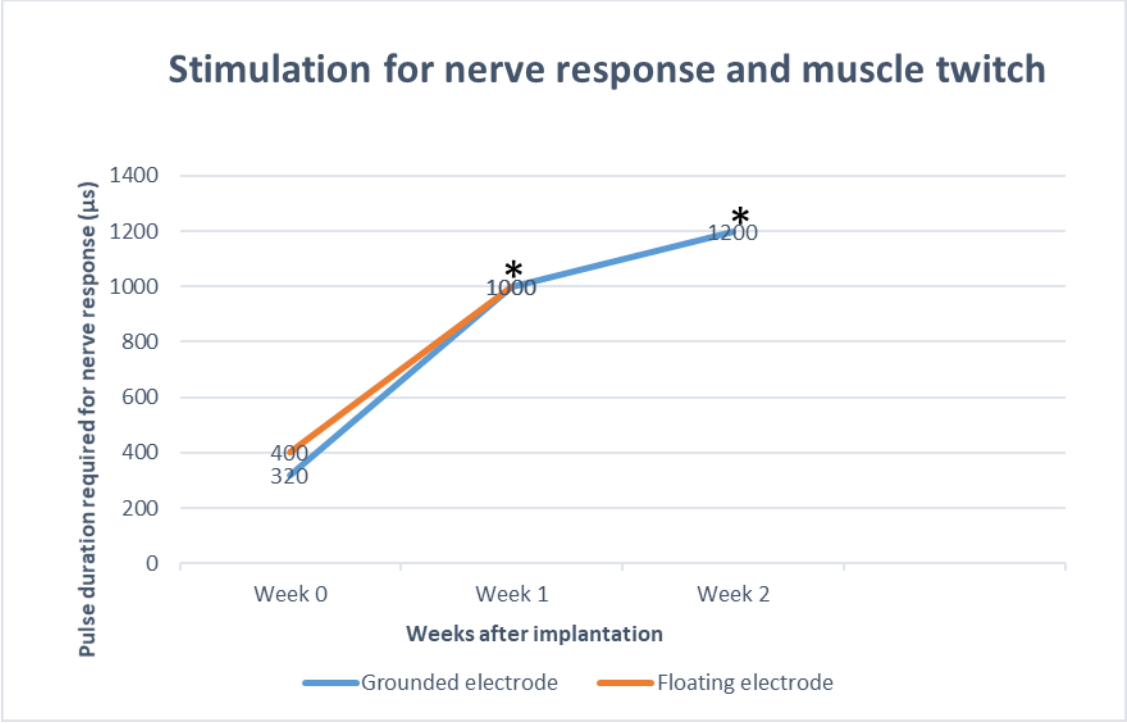

Figure 9. – Graphical representation of the change in minimum pulse duration required to trigger threshold nerve potentials in the rat sciatic nerve at a constant stimulation pulse amplitude of 250 µA with time for the electrode A (blue) and B (orange). * Time of electrode failure.

.3.2.2 Presence of scar tissue on uncoated implants after nerve harvesting procedure

After electrode failure of both implants, the wound incision from the implantation surgery was reopened for both rats, and the sciatic nerve and the uncoated electrodes were harvested (Figure 10). The electrodes A and B were extracted from the rats at weeks 2 and 3 respectively. During the nerve harvesting procedure, we observed that the two implants were fused to the surrounding muscles and connective tissues (Figure 10B). A thick fibrous membrane of connective tissue encapsulated the entire device, including the recording and stimulation wires of the implant. The wires connecting to the headstage on the rat skull were also covered with scar tissue and displayed signs of abrasions on their surfaces. We also verified that the stimulation and recording wires of the uncoated electrodes were still implanted into the rat sciatic nerve, showing that loss of electrode function was not due to electrode displacement, but most likely due to the progressive formation of scar tissue through FBR.

A)

B)

Figure 10. – A) Wound incision from the nerve harvesting surgery B) Presence of scar tissue on the uncoated electrodes after the nerve harvesting surgery at 3 weeks in the rat sciatic nerve.

Chapter 4 – Discussion

.4 Discussion

.4.1 Coated microsphere in vivo experiment

Peripheral nerve implants have the potential to help upper-limb amputees restore sensory feedback, regain motor function and manage complications, such as phantom-limb pain. However, FBR greatly reduces the long-term function of these implants and limits their clinical application in the PNS. We propose the novel strategy of using synapse-promoting polymers, such as DND and PDL, to reduce the effect of FBR on peripheral nerve implants. Previous studies from our laboratory have shown that DND and PDL are able to induce the formation of synaptic contacts from human IPSC-derived motor neurons in vitro. Furthermore, live-cell imaging showed that these synapses appear to be functional, and DND-coated microbeads had greater synaptophysin accumulation around them 2 weeks after injection into rat sciatic nerve, than is found around CTRL or PDL beads (Ma et al., 2018). As a continuation of that study, my masters' project sought to determine whether DND and PDL could also promote the accumulation of synaptic proteins in rat sciatic nerve at longer time points (4, 6 and 8 weeks), and whether or not DND is more synaptogenic than PDL, as is seen in vitro. This is an important step before testing these synthetic coatings on the surface of peripheral nerve implants. My results from these experiments show that DND and PDL do promote the formation of presynaptic complexes on microbeads at 4, 6 and 8 weeks in vivo. In addition, I observed greater accumulation of these complexes around DND-coated beads than either PDL or CTRL beads, and the accumulation of synaptophysin around DND-coated beads is significantly higher than around CTRL beads at all time points, indicating that these complexes are at least stable for up to 8 weeks in the rat sciatic nerve.

.4.1.1 DND and PDL can promote the formation of presynaptic elements on microbeads in vivo

A nerve crush injury model of the rat was used to evaluate the synapse-promoting properties of DND and PDL at 4, 6 and 8 weeks in vivo. Consistent with previous studies completed by our laboratory and our collaborators (Lucido et al., 2010; Lucido et al., 2009; Ma et al., 2018) (Al-

Alwan et al. unpublished data), our results suggest that DND and PDL can induce the formation of presynaptic elements on microspheres in the PNS. In confocal images, we observed the formation of synaptophysin-positive puncta on the surface of DND-coated and PDL-coated microbeads in the rat sciatic nerve (Figure 2). When these synaptophysin puncta were quantified, a significantly higher accumulation of synaptophysin was observed on the surface of DND-coated microbeads compared to uncoated beads for the crush site at 4 and 6 weeks ($p \leq 0.05$, $p \leq 0.001$ respectively) and for the distal site at 4, 6 and 8 weeks ($p \leq 0.01$, $p \leq 0.0001$, $p \leq 0.05$ respectively) (Figure 3A, B and C). PDL-coated microbeads also had a significantly higher accumulation of synaptophysin puncta on their surface compared to CTRL beads at 6 weeks for the distal site ($p \leq 0.05$) (Figure 3B). These findings show that both PDL and DND can promote higher synaptophysin accumulation on microbeads compared to CTRL in the rat sciatic nerve. Considering that the synaptophysin protein plays an important role in synaptic functions in the CNS (Glantz et al., 2007), the observation of synaptophysin accumulation on PDL-coated and DND-coated microbeads suggest that these may represent the formation of presynaptic elements on the microbead surface. These findings propose that the synapse-promoting property of DND found in previous in vitro microbead studies translates to an in vivo model (Richard W. Burry, 1980, 1982; Richard W. Burry, 1983; R. W. Burry et al., 1986; R.W. Burry et al., 1986; Lucido et al., 2010; Lucido et al., 2009; Ma et al., 2018).

Previous in vitro studies using both IPSC-derived motor and hippocampal neurons have also showed that DND induces more robust accumulation of synaptophysin around microbeads than PDL and CTRL (Al-Alwan et al, unpublished data; Ma et al, 2018). To study this process in vivo in the rat sciatic nerve, I compared the synaptophysin accumulation found on DND-coated and PDL-coated microbeads at 4, 6 and 8 weeks post-injection. Consistent with the previous in vitro studies my results show that DND-coated microbeads had a significantly higher amount of synaptophysin accumulation compared to PDL-coated microbeads at 4 weeks for the distal site ($p \leq 0.01$) (Figure 3A). DND-coated beads also consistently demonstrated more robust synaptophysin accumulation compared to PDL-coated microbeads at the other tested timepoints (6 and 8 weeks) (Figure 3B and C), even though the synaptophysin values were not significantly different between the

conditions. These results show that DND is better than PDL at inducing the accumulation of synaptophysin on microbeads in vivo.

Although the mechanism of action for DND has not yet been elucidated, we hypothesize that the surface charge present on DND could play an important role in its synaptogenic property. Based on previous studies showing that DND has amine groups on its surface (Hellmund et al., 2015; Hellmund et al., 2014), we speculate that DND uses these functional groups to interact closely with the axonal membrane of the nerve and induce presynaptic formation. This hypothesis is supported by previous CNS studies, which have shown that electrostatic interactions between the postsynaptic and presynaptic elements are necessary for the initiation of synaptogenesis (Hellmund et al., 2015; Hellmund et al., 2014), we speculate that DND uses these functional groups to interact closely with the axonal membrane of the nerve and cause presynaptic formation. This hypothesis is supported by previous CNS studies, which have shown that electrostatic interactions between the postsynaptic and presynaptic elements are necessary for the initiation of synaptogenesis (R. W. Burry et al., 1978; Pfenninger, 1971). Furthermore, spherical supported bilayer lipid membranes (SS-BLMs) with primary amine moieties on their surface have been shown to induce the formation of presynaptic elements on silica beads but not when these amine groups were absent (Gopalakrishnan et al., 2010). This would support our hypothesis that the positive surface charge found on the DND polymer allows it to form a strong adhesion between the microbead and the axonal membrane. To confirm this mechanism, more research would need to be completed.

Moreover, the PDL-coated beads did not show significant accumulation of synaptophysin at most of the tested time points and nerve sites when compared to the CTRL group (Figure 3). Although PDL has shown to induce synapse formation in vitro when coated onto microbeads, this does not appear to happen as well in vivo (Ma et al., 2018). One possible explanation for this is that the PDL coating may have dissolved over time from the microbead surface. This mechanism was suggested in a study examining the effect of PDL that were physically- and covalently-coated onto substrates for neuronal cell adhesion (Kim et al., 2011). The study showed that after 20 days of incubation, cultured neuronal cells stripped away from ITO substrate that was physically-coated with PDL. It is possible that a similar process might have occurred in our study as the PDL-coated

microbeads were incubated with peripheral neurons for more than 28 days (4 weeks). The dissolution of PDL could have led to weakened interaction and detachment of synaptophysin puncta from the PDL-coated microbeads, thereby decreasing the synaptophysin accumulation values obtained at 4, 6 and 8 weeks. This may explain why PDL has a less stable synapse-promoting property compared to DND at 4, 6 and 8 weeks in vivo

.4.1.2 Time-course of synaptophysin accumulation on microbeads at 4, 6 and 8 weeks in vivo

To evaluate the synapse-promoting property of PDL and DND on microbeads over time, I looked at the change in synaptophysin accumulation on microbeads coated with DND and PDL at 4, 6 and 8 weeks (Figure 4A and B). From this analysis, we showed that DND promoted stable synaptophysin accumulation on microbeads at 4 and 6 weeks for the crush site ($p \leq 0.05$, $p \leq 0.001$ respectively) and at 4, 6 and 8 weeks for the distal site ($p \leq 0.01$, $p \leq 0.0001$, $p \leq 0.05$ respectively) (Figure 4A and B). In comparison, the synaptophysin accumulation found for the PDL group did not differ significantly from the CTRL group at 4, 6 and 8 weeks ($p > 0.05$), except at 6 weeks for the distal site ($p \leq 0.05$) (Figure 4B). These results suggest that DND is a more stable and long-lasting synaptogenic polymer compared to PDL in vivo. When the conditions were compared to each other, higher synaptophysin accumulation values were also found for DND-coated microbeads compared to PDL-coated microbeads at 4 weeks for the distal site ($p \leq 0.01$) (Figure 4A and B). Consistent with previous in vitro studies (Al-Alwan et al. unpublished data), these results suggest that DND has a superior synapse-promoting property compared to PDL.

The synaptophysin accumulation for the DND group at the crush site dropped to baseline values at 8 weeks ($p > 0.05$), although significantly higher than the CTRL group at 4 and 6 weeks ($p \leq 0.05$, $p \leq 0.001$ respectively) (Figure 4A). However, at 8 weeks, there was still significantly higher synaptophysin accumulation around DND-coated beads at the distal site ($p \leq 0.05$) (Figure 4B). It is possible that the regenerating axons of the injured nerve have grown past the crush site at 8 weeks and are forming new neuronal processes and outgrowths at the distal site. Following nerve injury, the peripheral nerve enters a regenerative state and will begin regenerating from the proximal site of the injury to the distal site (Huebner et al., 2009; Sulaiman et al., 2013). It is possible that at the 8-week timepoint, presynaptic elements formed on PDL and DND-coated microbeads at the crush site could have undergone the process of synaptic pruning as the nerve

regeneration continued onto the distal site. Another possibility is that without any postsynaptic elements on the surface of the bead, the non-functional presynaptic elements formed on the bead surface could have degenerated or been removed by the PNS. These mechanisms were also suggested by previous CNS studies demonstrating a similar decline in presynaptic elements on poly-L-lysine-coated microbeads after 7-9 days of incubation in vitro and 14-21 days in vivo (Richard W. Burry, 1982; R. W. Burry et al., 1986). Whether or not this will also occur in an amputated nerve will have to be studied in the future.

.4.1.3 Bead distributions for PDL, DND and CTRL groups at 4, 6 and 8 weeks

To compare the synaptogenic effect of DND and PDL on microbeads, we also looked at the frequency of microbeads with two synaptophysin puncta or more in the CTRL, DND and PDL groups at 4, 6 and 8 weeks. Our results showed that the frequency of microbeads with two synaptophysin puncta or more were higher for the DND group compared to the CTRL group at 4 and 6 weeks for both crush and distal sites ($p \leq 0.05$) (Figure 5A and B). In contrast, the bead distribution for the PDL group did not differ significantly from the CTRL group at 4, 6 and 8 weeks ($p > 0.05$). These findings suggest that a higher frequency of microbeads in the DND group has an elevated synaptophysin puncta number on their surface compared to the CTRL group. This finding further supports our hypothesis that DND can promote the significant formation of presynaptic elements on microbeads at 4, 6 and 8 weeks in vivo.

.4.2 Uncoated electrode in vivo experiment

Many electrode designs have been used for the study of spinal cord injuries and upper-limb amputations, including cuff electrodes, intraneural electrodes and regenerative electrodes. However, no standard implant model has been developed to assess the long-term signal stability of peripheral nerve implants in the body. The purpose of my uncoated electrode in vivo experiment is to establish an electrode design that can be used to study the effect of PDL and DND on the long-term performance of these devices in vivo in a future experiment. To accomplish this objective, I made an electrode construct with a recording and stimulation wire and tested its function in a rat sciatic nerve model. This construct was successfully tested in a live rat, and I was

able to continue recording and stimulating from the implanted electrode for several weeks until electrode failure.

.4.2.1 Our electrode set-up can record and stimulation nerve potentials from the nerve

Using the Multichannel W2100 System, I conducted electrophysiological recordings on rats implanted with the intraneural electrode every week and measured the signal stability of the implant over time. My results showed that on the day of the implantation, the uncoated electrodes could stimulate and record nerve signals from the rat sciatic nerve using stimulations at varying pulse amplitudes and durations (Appendix Figure 10). The electrodes A and B could also perform nerve recordings in the rat for one week and two weeks respectively before not being able to record any nerve signals (Appendix Figure 11 and 12). These observations show that this electrode set-up is functional and can acquire neural information from the rat sciatic nerve. To assess the signal stability of these electrodes, I also measured the minimum pulse duration required to trigger a threshold nerve potential every week (Appendix Figure 8). Other studies have used a similar measurement to assess the long-term function of their implant. For example, a study tested the signal stability of a nerve cuff electrode by measuring the minimum stimulation charge required to trigger a visible muscle contraction in a patient's quadriceps (Fisher et al., 2009). This validates the procedure that we have been using for our electrode model. Thus, we can conclude that our intraneural electrode is functional and can be used to assess the long-term performance of peripheral nerve implants in vivo.

.4.2.2 Foreign body reaction reduced the function and lifetime of our uncoated implants

Although the electrode set-up was shown to be functional, I observed that the signal stability of these two electrodes started to degrade within the first week of recording. At week 1 post-implantation, the pulse duration required to trigger a threshold nerve potential increased from 320 µs to 1000 µs for the electrode A (Appendix Figure 8). As for electrode B, the pulse duration increased from 400 µs to 1000 µs (Appendix Figure 8). A similar result was observed in a study that used tf-LIFE electrodes to restore sensations in a patient with an upper-limb amputation. They showed that the minimum stimulation charge required to trigger sensations in a patient's phantom limb increased from 0.1 nC to 1 nC in the first ten days (Rossini et al., 2010). One

explanation for the increased pulse requirement observed in our experiment is that the FBR process affected the function of the recording or stimulation wires of our electrodes (de la Oliva, Navarro, et al., 2018; Vasudevan et al., 2017; Wurth et al., 2017). This hypothesis is supported by the fact that I observed a thick tissue capsule surrounding the intraneural implants during the nerve harvesting procedure (Appendix Figure 9). The recording and stimulation wires of the implant were also covered with scar tissue. Moreover, previous studies have reported that fibrous tissue could encapsulate polyimide-based intraneural electrodes and reduce their function within the first week of implantation (de la Oliva, Navarro, et al., 2018; Vasudevan et al., 2017; Wurth et al., 2017). This fibrotic reaction likely contributed to the requirement of increased pulse duration over time to stimulate the nerve, as was observed in my experiment.

Furthermore, these results also showed that the uncoated electrodes were not very long-lasting. The electrode A and B could no longer acquire any nerve signal or trigger any muscle twitch from the rat after 2 and 3 weeks respectively (Appendix Figure 8). One possible explanation for this observation would be that the recording or stimulation wires of our implant were broken or displaced in the rat sciatic nerve. A similar outcome has previously occurred in other intraneural electrodes used for rats and humans (Davis et al., 2016; Malaga et al., 2016; Petrini et al., 2019; Vasudevan et al., 2017). However, I found that the recording and stimulation wires were still secured to the sciatic nerve during the nerve harvesting procedure. Another possible explanation would be that the FBR process decreased the function of our uncoated electrodes to the extent that no biological response could be recorded. This hypothesis would be supported by the fact that there was visual evidence of extensive FBR on our uncoated electrodes after the harvesting procedure (Appendix Figure 9). Fibrous tissue also encapsulated the recording and stimulation wires in the implant and contributed to the increased pulse duration observed for these electrodes. From these observations, I conclude that FBR can greatly reduce the function and the lifetime of the PNS implant. There is a significant need for a more biocompatible electrode design, which would limit FBR and allow the electrodes to function over a longer period of time. It is possible that coating the electrode with a synaptogenic substance, such as DND, may allow the peripheral nerves to form synaptic contacts with the surface of the electrodes, and therefore decrease the amount of FBR.

.4.3 Future research

In the future, it would be interesting to test whether DND or PDL can actually reduce FBR in the body and improve the signal stability and lifetime of peripheral nerve implants using our electrode model. The results of this future study would have profound implications for the field of neuroprosthetics and the treatment of upper-limb amputation. In subsequent studies, it would be also interesting to examine whether other types of dendrimers or poly-basic substances could be used to promote the formation of presynaptic elements on microbeads in the PNS and CNS. The synthetic polymers could also have synaptogenic properties that we can use to improve the biocompatibility of implants. Potential candidates for these experiments include polyamidoamine (PAMAM), poly(propylene) imine (PEI) and PPI (Hellmund et al., 2015).

Furthermore, the synapse-promoting properties of PDL and DND have been only tested on the spherical surface of microbeads in past CNS and PNS studies (Lucido et al., 2010; Lucido et al., 2009; Ma et al., 2018) (Al-Alwan et al. unpublished data). Future experiments should explore whether the synapse-promoting effect of these synthetic polymers could be used for other types of surfaces. This consideration is important considering that some shapes, such as triangular-shaped objects, can trigger the formation of scar tissue more than others (Matlaga et al., 1976). These results will inform us whether a microbead surface needs to be implemented into the design of future peripheral nerve implants for the application of these synthetic polymers. Moreover, despite the extensive research completed by our collaborators on DND (Hellmund et al., 2015; Hellmund et al., 2014; R. K. Kainthan et al., 2007; Rajesh Kumar Kainthan et al., 2006; Kurniasih et al., 2015; Adam L. Sisson et al., 2010; A. L. Sisson et al., 2009), the mechanism of action through which DND can promote the formation of presynaptic complexes on microbeads remains unclear in the PNS and CNS. We have suggested a few possibilities for the synapse-promoting property of DND in our study. It would be relevant to test these hypotheses in subsequent studies to better understand the process of synapse formation on artificial surfaces.

In the uncoated electrode in vivo experiment, we also did not have the opportunity to characterize the presence of scar tissue and fibrotic reaction in the body for our uncoated electrodes using different qualitative or quantitative measures, such as capsule thickness, cell composition, nerve myelination and collagen aggregation. These metrics have been used

previously to study the consequences of FBR on intraneural electrodes (de la Oliva, Navarro, et al., 2018; Wurth et al., 2017). For subsequent research, it would be relevant to include these tests so that we can have a better idea of what is occurring in the peripheral nerve implants after the implantation surgery. Electrical impedance measurements, locomotor tasks and sham surgeries should also be included in future experimental designs. These measures will help us better define the effect of FBR on the long-term function of peripheral nerve implants.

.4.4 Clinical Implications

Our coated microsphere in vivo experiment shows that DND and PDL can promote the formation of presynaptic elements on the surface of polystyrene microbeads from 4 weeks to 8 weeks post-injection into rat sciatic nerve. This study addresses a major gap that exists in the literature concerning whether the synaptogenic properties of PDL and DND can translate to an in vivo model in the PNS and whether the effect is long-lasting. Most of the previous work done on these two synthetic polymers were completed in the CNS using in vitro models (Lucido et al., 2010; Lucido et al., 2009)(Al-Alwan et al. unpublished data). This study demonstrates that these synthetic coatings can induce the formation of synaptic contacts between an artificial surface and the PNS of the rat. These findings support the possibility of coating DND and PDL onto the surface of peripheral nerve implants and inducing the formation of presynaptic elements on them. The next step will be to test whether the synapse-promoting properties of these synthetic polymers can improve the signal stability and long-term function of peripheral nerve implants through reducing FBR in the body. From previous studies, it is known that FBR can greatly increase the electrical impedance and increase the stimulation charge required to trigger nerve response in (Wurth et al. 2017; Rossini et al. 2010; Petrini et al., 2019) Our uncoated electrode in vivo experiment further supports this idea by showing that FBR can promote scar tissue formation around intraneural electrodes and reduce their function within the first week of implantation. These findings support the use of synthetic polymers, such as DND and PDL, to improve the surface properties of these implants.

Chapter 5 – Conclusion

.5 Conclusion

In conclusion, the coated microsphere in vivo study shows for the first time that DND and PDL can promote the formation of stable presynaptic elements on microbeads at 4, 6 and 8 weeks in an animal model. Our results also demonstrate that DND is a superior and more stable synapse-promoting molecule compared to PDL as shown by the higher synaptophysin accumulation on DND-coated vs. PDL-coated microbeads at 4 weeks for the distal site. As for the uncoated electrode in vivo study, our results show that our electrode system is functional and can record nerve signals from the rat sciatic nerve for one to two weeks. However, the implant is not long-lasting in the body due to the effect of FBR, which decreases the signal stability and lifetime of our implant. I believe that our proposed approach of using DND and PDL to induce the formation of presynaptic elements on artificial surfaces is feasible and that we now have an electrode model on which we can test the effect of these synthetic polymers in vivo. If we can show that DND and PDL can reduce the effect of FBR on peripheral nerve implants in a future study, this coating technology may help make PNS implants more long-lasting, which would have great clinical significance.

Acknowledgements

The author would like to thank Michel Paquet and Timothy Lan Chung Yang for their technical assistance in the experiments, as well as Elke Kuster from the plateforme d'imagerie microscopique (PIM) and Ricardo Claudio from the animal care facility at CHU Sainte-Justine. The author is also grateful to Dr. Timothy E. Kennedy for allowing him to use his lab at the Montreal Neurological Institute for the project. This project is funded by a joint grant from the Natural Sciences and Engineering Research Council (NSERC) and the Canadian Institutes of Health Research (CIHR). Also, this scholarship is funded by the TransMedTech Institute and its main funding partner, the Canada First Research Excellence Fund. The author was also supported by the Faculté des études supérieures postdoctorales de l'Université de Montréal (FESP).

References

Ahmari, S. E., & Smith, S. J. (2002). Knowing a Nascent Synapse When You See It. *Neuron, 34*, 333–336. doi:10.1016/s0896-6273(02)00685-2

Amaral, E., Guatimosim, S., & Guatimosim, C. (2011). Using the Fluorescent Styryl Dye FM1-43 to Visualize Synaptic Vesicles Exocytosis and Endocytosis in Motor Nerve Terminals. In H. Chiarini-Garcia & R. Melo (Eds.), *Light Microscopy. Methods in Molecular Biology (Methods and Protocols)* (Vol. 689, pp. 137-148). Totowa, NJ: Humana Press.

Aregueta-Robles, U. A., Woolley, A. J., Poole-Warren, L. A., Lovell, N. H., & Green, R. A. (2014). Organic electrode coatings for next-generation neural interfaces. *Front Neuroeng, 7*, 15. doi:10.3389/fneng.2014.00015

Arvidsson U., Riedl M., Elde R., & Meister B. (1997). Vesicular acetylcholine transporter (VAChT) protein: a novel and unique marker for cholinergic neurons in the central and peripheral nervous systems. *J Comp Neurol, 378*(4), 454-467.

Baron, R., Binder, A., & Wasner, G. (2010). Neuropathic pain: diagnosis, pathophysiological mechanisms, and treatment. *Lancet Neurol, 9*(8), 807-819. doi:10.1016/S1474-4422(10)70143-5

Bhuvaneswar, C. G., Epstein, L. A., & Stern, T. A. (2007). Reactions to amputation: recognition and treatment. . *Primary care companion to the Journal of clinical psychiatry, 9*, 303–308. doi:10.4088/pcc.v09n0408

Biddiss, E., & Chau, T. (2007). Upper-limb prosthetics: critical factors in device abandonment. *Am J Phys Med Rehabil, 86*(12), 977-987. doi:10.1097/PHM.0b013e3181587f6c

Branner, A., Stein, R. B., Fernandez, E., Aoyagi, Y., & Normann, R. A. (2004). Long-term stimulation and recording with a penetrating microelectrode array in cat sciatic nerve. *IEEE Trans Biomed Eng, 51*(1), 146-157. doi:10.1109/TBME.2003.820321

Bridge, P. M., Ball, D. J., Mackinnon, S. E., Nakao, Y., Brandt, K., Hunter, D. A., & Hertl, C. (1994). Nerve Crush Injuries—A Model for Axonotmesis. *Experimental Neurology, 127* (2), 284-290

doi:10.1006/exnr.1994.1104

Brown, J. D., Paek, A., Syed, M., O'Malley, M. K., Shewokis, P. A., Contreras-Vidal, J. L., . . . Gillespie, R. B. (2015). An exploration of grip force regulation with a low-impedance myoelectric prosthesis featuring referred haptic feedback. *Journal of NeuroEngineering and Rehabilitation, 12*(1), 104. doi:10.1186/s12984-015-0098-1

Burry, R. W. (1980). Formation Of Apparent Presynaptic Elements In Response To Poly-Basic Compounds. *Brain Research Protocols, 184*, 85-98. doi:10.1016/0006-8993(80)90588-0

Burry, R. W. (1982). Development of Apparent Presynaptic Elements Formed in Response to Polylysine Coated Surfaces. *Brain Research Protocols, 247*, 1-16. doi:10.1016/0006-8993(82)91022-8

Burry, R. W. (1983). Postnatal rat neurons form apparent presynaptic elements on polylysine-coated beads in vivo. *Brain Research, 278*(1-2), 236-239. doi:10.1016/0006-8993(83)90244-5

Burry, R. W., & Hayes, D. M. (1986). Development and Elimination of Presynaptic Elements on Polylysine-Coated Beads Implanted in Neonatal Rat Cerebellum. *Journal of Neuroscience Research, 15*, 67-78. doi:10.1002/jnr.490150107

Burry, R. W., Ho, R. H., & Matthew, W. D. (1986). Presynaptic elements formed on polylysine-coated beads contain synaptic vesicle antigens *J Neurocytol, 15*(4), 409-419. doi:10.1007/BF01611725

Burry, R. W., & Lasher, R. S. (1978). A quantitative electron microscopic study of synapse formation in dispersed cell cultures of rat cerebellum stained either by Os-UL or by E-PTA. *Brain Research, 147*(1), 1-15. doi:10.1016/0006-8993(78)90768-0

Calhoun, M. E., Jucker, M., Martin, L. J., Thinakaran, G., Price, D. L., & Mouton, P. R. (1996). Comparative evaluation of synaptophysin-based methods for quantification of synapses. *Journal of Neurocytology 25*, 821-828 doi:10.1007/BF02284844

Cheesborough, J. E., Smith, L. H., Kuiken, T. A., & Dumanian, G. A. (2015). Targeted muscle reinnervation and advanced prosthetic arms. *Semin Plast Surg, 29*(1), 62-72. doi:10.1055/s-0035-1544166

Ciancio, A. L., Cordella, F., Barone, R., Romeo, R. A., Bellingegni, A. D., Sacchetti, R., . . . Zollo, L. (2016). Control of Prosthetic Hands via the Peripheral Nervous System. *Front Neurosci, 10*, 116. doi:10.3389/fnins.2016.00116

Cracchiolo, M., Valle, G., Petrini, F., Strauss, I., Granata, G., Stieglitz, T., . . . Micera, S. (2020). Decoding of grasping tasks from intraneural recordings in trans-radial amputee. *J Neural Eng, 17*(2), 026034. doi:10.1088/1741-2552/ab8277

D'Anna, E., Valle, G., Mazzoni, A., Strauss, I., Iberite, F., Patton, J., . . . Micera, S. (2019). A closed-loop hand prosthesis with simultaneous intraneural tactile and position feedback. *Science Robotics, 4*(27), eaau8892. doi:10.1126/scirobotics.aau8892

Darnall, B. D., Ephraim, P., Wegener, S. T., Dillingham, T., Pezzin, L., Rossbach, P., & MacKenzie, E. J. (2005). Depressive symptoms and mental health service utilization among persons with limb loss: Results of a national survey. *Archives of Physical Medicine and Rehabilitation, 86,*(4), 650-658. doi:10.1016/j.apmr.2004.10.028

Davis, T. S., Wark, H. A., Hutchinson, D. T., Warren, D. J., O'Neill, K., Scheinblum, T., . . . Greger, B. (2016). Restoring motor control and sensory feedback in people with upper extremity amputations using arrays of 96 microelectrodes implanted in the median and ulnar nerves. *J Neural Eng, 13*(3), 036001. doi:10.1088/1741-2560/13/3/036001

de la Oliva, N., Mueller, M., Stieglitz, T., Navarro, X., & Del Valle, J. (2018). On the use of Parylene C polymer as substrate for peripheral nerve electrodes. *Sci Rep, 8*(1), 5965. doi:10.1038/s41598-018-24502-z

de la Oliva, N., Navarro, X., & Del Valle, J. (2018). Time course study of long-term biocompatibility and foreign body reaction to intraneural polyimide-based implants. *J Biomed Mater Res A, 106*(3), 746-757. doi:10.1002/jbm.a.36274

Deng, L., Kaeser, P. S., Xu, W., & Südhof, T. C. (2011). RIM proteins activate vesicle priming by reversing autoinhibitory homodimerization of Munc13. . *Neuron, 69*(2), 317-331. doi:10.1016/j.neuron.2011.01.005

Desmond, D. M. (2007). Coping, affective distress, and psychosocial adjustment among people with traumatic upper limb amputations. *J Psychosom Res, 62*(1), 15-21. doi:10.1016/j.jpsychores.2006.07.027

Dhillon, G. S., & Horch, K. W. (2005). Direct neural sensory feedback and control of a prosthetic arm. *IEEE Trans Neural Syst Rehabil Eng, 13*(4), 468-472. doi:10.1109/TNSRE.2005.856072

Dhillon, G. S., Kruger, T. B., Sandhu, J. S., & Horch, K. W. (2005). Effects of short-term training on sensory and motor function in severed nerves of long-term human amputees. *J Neurophysiol, 93*(5), 2625-2633. doi:10.1152/jn.00937.2004

Dhillon, G. S., Lawrence, S. M., Hutchinson, D. T., & Horch, K. W. (2004). Residual function in peripheral nerve stumps of amputees: implications for neural control of artificial limbs. *J Hand Surg Am, 29*(4), 605-615; discussion 616-608. doi:10.1016/j.jhsa.2004.02.006

Dickinson, B. D., Head, C. A., Gitlow, S., & Osbahr, A. J. r. (2010). Maldynia: pathophysiology and management of neuropathic and maladaptive pain--a report of the AMA Council on Science and Public Health. *Pain Med, 11*(11), 1635-1653. doi:10.1111/j.1526-4637.2010.00986.x

Eggers, T. E., Dweiri, Y. M., McCallum, G. A., & Durand, D. M. (2018). Recovering Motor Activation with Chronic Peripheral Nerve Computer Interface. *Sci Rep, 8*(1), 14149. doi:10.1038/s41598-018-32357-7

Fernández, A., Isusi, I., & Gómez, M. (2000). Factors conditioning the return to work of upper limb amputees in Asturias, Spain. *Prosthetics and Orthotics International 24*(2), 143-147. doi:10.1080/03093640008726537

Fisher, L. E., Tyler, D. J., Anderson, J. S., & Triolo, R. J. (2009). Chronic stability and selectivity of four-contact spiral nerve-cuff electrodes in stimulating the human femoral nerve. *J Neural Eng, 6*(4), 046010. doi:10.1088/1741-2560/6/4/046010

George, J. A., Kluger, D. T., Davis, T. S., Wendelken, S. M., Okorokova, E. V., He, Q., . . . Clark, G. A. (2019). Biomimetic sensory feedback through peripheral nerve stimulation improves dexterous use of a bionic hand. *Science Robotics, 4*(32), eaax2352. doi:10.1126/scirobotics.aax2352

Glantz, L. A., Gilmore, J. H., Hamer, R. M., Lieberman, J. A., & Jarskog, L. F. (2007). Synaptophysin and postsynaptic density protein 95 in the human prefrontal cortex from mid-gestation into early adulthood. *Neuroscience, 149*(3), 582–591. doi:10.1016/j.neuroscience.2007.06.036

Gopalakrishnan, G., Thostrup, P., Rouiller, I., Lucido, A. L., Belkaid, W., Colman, D. R., & Lennox, R. B. (2010). Lipid bilayer membrane-triggered presynaptic vesicle assembly. *ACS Chem Neurosci, 1*(2), 86-94. doi:10.1021/cn900011n

Graczyk, E. L., Resnik, L., Schiefer, M. A., Schmitt, M. S., & Tyler, D. J. (2018). Home Use of a Neural-connected Sensory Prosthesis Provides the Functional and Psychosocial Experience of Having a Hand Again. *Sci Rep, 8*(1), 9866. doi:10.1038/s41598-018-26952-x

Granata, G., Di Iorio, R., Romanello, R., Iodice, F., Raspopovic, S., Petrini, F., . . . Rossini, P. M. (2018). Phantom somatosensory evoked potentials following selective intraneural electrical stimulation in two amputees. *Clin Neurophysiol, 129*(6), 1117-1120. doi:10.1016/j.clinph.2018.02.138

Gundelfinger, E. D., Reissner, C., & Garner, C. C. (2016). Role of Bassoon and Piccolo in Assembly and Molecular Organization of the Active Zone. *Frontiers in synaptic neuroscience, 7*, 19. doi:10.3389/fnsyn.2015.00019

Hellmund, M., Achazi, K., Neumann, F., Thota, B. N., Ma, N., & Haag, R. (2015). Systematic adjustment of charge densities and size of polyglycerol amines reduces cytotoxic effects and enhances cellular uptake. *Biomater Sci, 3*(11), 1459-1465. doi:10.1039/c5bm00187k

Hellmund, M., Zhou, H., Samsonova, O., Welker, P., Kissel, T., & Haag, R. (2014). Functionalized polyglycerol amine nanogels as nanocarriers for DNA. *Macromol Biosci, 14*(9), 1215-1221. doi:10.1002/mabi.201400144

Horch, K., Meek, S., Taylor, T. G., & Hutchinson, D. T. (2011). Object discrimination with an artificial hand using electrical stimulation of peripheral tactile and proprioceptive pathways with intrafascicular electrodes. *IEEE Trans Neural Syst Rehabil Eng, 19*(5), 483-489. doi:10.1109/TNSRE.2011.2162635

Huebner, E. A., & Strittmatter, S. M. (2009). Axon regeneration in the peripheral and central nervous systems. *Results Probl Cell Differ, 48*, 339-351. doi:10.1007/400_2009_19

Iwabuchi S., Kakazu Y., Koh J.Y., Goodman K.M., & Harata N.C. (2014). Examination of synaptic vesicle recycling using FM dyes during evoked, spontaneous, and miniature synaptic activities. *J Vis Exp*(85), 505-557. doi:10.3791/50557

Jahn, R., Schiebler, W., Ouimet, C., & Greengard, P. . (1985). A 38,000-dalton membrane protein (p38) present in synaptic vesicles. *Proceedings of the National Academy of Sciences of the United States of America, 82*(12), 4137–4141. doi:10.1073/pnas.82.12.4137

Kainthan, R. K., & Brooks, D. E. (2007). In vivo biological evaluation of high molecular weight hyperbranched polyglycerols. *Biomaterials, 28*(32), 4779-4787. doi:10.1016/j.biomaterials.2007.07.046

Kainthan, R. K., Janzen, J., Levin, E., Devine, D. V., & Brooks, D. E. (2006). Biocompatibility Testing of Branched and Linear Polyglycidol. *Biomacromolecules, 7*(3), 703-709. doi:10.1021/bm0504882

Kaur, A., & Guan, Y. (2018). Phantom limb pain: A literature review. *Chin J Traumatol, 21*(6), 366-368. doi:10.1016/j.cjtee.2018.04.006

Kim, Y. H., Baek, N. S., Han, Y. H., Chung, M. A., & Jung, S. D. (2011). Enhancement of neuronal cell adhesion by covalent binding of poly-D-lysine. *J Neurosci Methods, 202*(1), 38-44. doi:10.1016/j.jneumeth.2011.08.036

Krassioukov, A. V. (2002). Peripheral Nervous System. In R. V. S. (Ed.), *Encyclopedia of the Human Brain* (Vol. 1, pp. 817-830): Academic Press.

Kuiken, T. A., Barlow, A. K., Hargrove, L., & Dumanian, G. A. (2017). Targeted Muscle Reinnervation for the Upper and Lower Extremity. *Tech Orthop, 32*(2), 109-116. doi:10.1097/BTO.0000000000000194

Kurniasih, I. N., Keilitz, J., & Haag, R. (2015). Dendritic nanocarriers based on hyperbranched polymers. *Chem Soc Rev, 44*(12), 4145-4164. doi:10.1039/c4cs00333k

Lewis, S., Russold, M. F., Dietl, H., & Kaniusas, E. (2012). User demands for sensory feedback in upper extremity prostheses. *IEEE Xplore*.

Lotti, F., Ranieri, F., Vadala, G., Zollo, L., & Di Pino, G. (2017). Invasive Intraneural Interfaces: Foreign Body Reaction Issues. *Front Neurosci, 11*, 497. doi:10.3389/fnins.2017.00497

Lucido, A. L., Gopalakrishnan, G., Yam, P. T., Colman, D. R., & Lennox, R. B. (2010). Isolation of functional presynaptic complexes from CNS neurons: a cell-free preparation for the study of presynaptic compartments In vitro. *ACS Chem Neurosci, 1*(8), 535-541. doi:10.1021/cn100048z

Lucido, A. L., Suarez Sanchez, F., Thostrup, P., Kwiatkowski, A. V., Leal-Ortiz, S., Gopalakrishnan, G., . . . Colman, D. R. (2009). Rapid assembly of functional presynaptic boutons triggered by adhesive contacts. *J Neurosci, 29*(40), 12449-12466. doi:10.1523/JNEUROSCI.1381-09.2009

Ma, X., Al-Alwan, L., Larroquette, F., Clément, J.-P., Chitsaz, D., Fon, E., . . . Kennedy, T. E. (2018). *Enhancement of neural biocompatibility: Formation of Presynaptic Boutons on Cationic Polymer and Hyperbranched Polyglycerol-coated Microspheres in Peripheral Neurons.* (Maîtrise en sciences biomédicales, option médecine expérimentale). Université de Montréal, Papyrus.

Maduri, P., & Akhondi, H. (2020). Upper Limb Amputation. Retrieved from https://www.ncbi.nlm.nih.gov/books/NBK540962/

Malaga, K. A., Schroeder, K. E., Patel, P. R., Irwin, Z. T., Thompson, D. E., Nicole Bentley, J., . . . Patil, P. G. (2016). Data-driven model comparing the effects of glial scarring and interface interactions on chronic neural recordings in non-human primates. *J Neural Eng, 13*(1), 016010. doi:10.1088/1741-2560/13/1/016010

Markovic, M., Schweisfurth, M. A., Engels, L. F., Bentz, T., Wustefeld, D., Farina, D., & Dosen, S. (2018). The clinical relevance of advanced artificial feedback in the control of a multi-functional myoelectric prosthesis. *J Neuroeng Rehabil, 15*(1), 28. doi:10.1186/s12984-018-0371-1

Masliah, E., Fagan, A. M., Terry, R. D., DeTeresa, R., Mallory, M., & Gage, F. H. (1991). Reactive synaptogenesis assessed by synaptophysin immunoreactivity is associated with GAP-43 in the dentate gyrus of the adult rat. *Exp Neurol, 113*(2), 131-142. doi:10.1016/0014-4886(91)90169-d

Matlaga, B. F., Yasenchak, L. P., & Salthouse, T. N. (1976). Tissue Response to Implanted Polymers: The Significance of Sample Shape. *Journal of Biomedical Materials Research, 10*, 391-397 doi:10.1002/jbm.820100308

Menorca, R. M., Fussell, T. S., & Elfar, J. C. (2013). Nerve physiology: mechanisms of injury and recovery. *Hand Clin, 29*(3), 317-330. doi:10.1016/j.hcl.2013.04.002

Navone, F., Jahn, R., Di Gioia, G., Stukenbrok, H., Greengard, P., & De Camilli, P. (1986). Protein p38: An Integral Membrane Protein Specific for Small Vesicles of Neurons and Neuroendocrine Cells. *J Cell Biol., 103*(6), 2511-2527. doi:10.1083/jcb.103.6.2511

Oddo, C. M., Raspopovic, S., Artoni, F., Mazzoni, A., Spigler, G., Petrini, F., . . . Micera, S. (2016). Intraneural stimulation elicits discrimination of textural features by artificial fingertip in intact and amputee humans. *Elife, 5*, e09148. doi:10.7554/eLife.09148

Omar, A., Marwaha, K., & Bollu, P. C. (2020). Physiology, Neuromuscular Junction. Retrieved from https://www.ncbi.nlm.nih.gov/books/NBK470413/

Page, D. M., George, J. A., Kluger, D. T., Duncan, C., Wendelken, S., Davis, T., . . . Clark, G. A. (2018). Motor Control and Sensory Feedback Enhance Prosthesis Embodiment and Reduce Phantom Pain After Long-Term Hand Amputation. *Front Hum Neurosci, 12*, 352. doi:10.3389/fnhum.2018.00352

Peng, H., Cheng, P., & Luther, P. (1981). Formation of ACh receptor clusters induced by positively charged latex beads. *Nature 292*, 831–834. doi:10.1038/292831a0

Peng, H. B., & Cheng, P. C. (1982). Formation of postsynaptic specializations induced by latex beads in cultured muscle cells *The Journal of neuroscience : the official journal of the Society for Neuroscience, 2*(12), 1760–1774. doi:10.1523/JNEUROSCI.02-12-01760.1982

Peng, H. B., Markey, D. R., Muhlach, W. L., & Pollack, E. D. (1987). Development of Presynaptic Specializations Induced by Basic Polypeptide-Coated Latex Beads in Spinal Cord Cultures. *Synapse, 1*, 10-19. doi:10.1002/syn.890010104

Petrini, F. M., Valle, G., Strauss, I., Granata, G., Di Iorio, R., D'Anna, E., . . . Micera, S. (2019). Six-Month Assessment of a Hand Prosthesis with Intraneural Tactile Feedback. *Ann Neurol, 85*(1), 137-154. doi:10.1002/ana.25384

Pfenninger, K. H. (1971). The cytochemistry of synaptic densities. II. Proteinaceous components and mechanism of synaptic connectivity. *J Ultrastruct Res, 35*(5), 451-475. doi:10.1016/s0022-5320(71)80005-9

Ramachandran, V. S., Brang, D., & McGeoch, P. D. (2010). Dynamic reorganization of referred sensations by movements of phantom limbs. *Neuroreport, 21*(10), 727-730. doi:10.1097/WNR.0b013e32833be9ab

Raspopovic, S., Capogrosso, M., Petrini, F. M., Bonizzato, M., Rigosa, J., Di Pino, G., . . . Micera, S. (2014). Restoring Natural Sensory Feedback in Real-Time Bidirectional Hand Prostheses. *Science Translational Medicine, 6*(222), 222ra219-222ra219. doi:10.1126/scitranslmed.3006820

Raveh, E., Friedman, J., & Portnoy, S. (2018). Visuomotor behaviors and performance in a dual-task paradigm with and without vibrotactile feedback when using a myoelectric controlled hand. *Assist Technol, 30*(5), 274-280. doi:10.1080/10400435.2017.1323809

Rehm, H., Wiedenmann, B., & Betz, H. (1986). Molecular characterization of synaptophysin, a major calciumbinding protein of the synaptic vesicle membrane. *The EMBO Journal, 5*(3), 535-541.

Rijnbeek, E. H., Eleveld, N., & Olthuis, W. (2018). Update on Peripheral Nerve Electrodes for Closed-Loop Neuroprosthetics. *Front Neurosci, 12*, 350. doi:10.3389/fnins.2018.00350

Romero-Ortega, M. (2014). Peripheral Nerves, Anatomy and Physiology of. In *Encyclopedia of Computational Neuroscience* (pp. 1-5).

Rossini, P. M., Micera, S., Benvenuto, A., Carpaneto, J., Cavallo, G., Citi, L., . . . Dario, P. (2010). Double nerve intraneural interface implant on a human amputee for robotic hand control. *Clin Neurophysiol, 121*(5), 777-783. doi:10.1016/j.clinph.2010.01.001

Schiefer, M., Tan, D., Sidek, S. M., & Tyler, D. J. (2016). Sensory feedback by peripheral nerve stimulation improves task performance in individuals with upper limb loss using a myoelectric prosthesis. *J Neural Eng, 13*(1), 016001. doi:10.1088/1741-2560/13/1/016001

Sisson, A. L., & Haag, R. (2010). Polyglycerol nanogels: highly functional scaffolds for biomedical applications. *Soft Matter, 6*(20). doi:10.1039/c0sm00149j

Sisson, A. L., Steinhilber, D., Rossow, T., Welker, P., Licha, K., & Haag, R. (2009). Biocompatible functionalized polyglycerol microgels with cell penetrating properties. *Angew Chem Int Ed Engl, 48*(41), 7540-7545. doi:10.1002/anie.200901583

Slater, C. R. (2017). The Structure of Human Neuromuscular Junctions: Some Unanswered Molecular Questions. *International journal of molecular sciences, 18*(10), 2183. doi:10.3390/ijms18102183

Smail, L. C., Neal, C., Wilkins, C., & Packham, T. L. (2020). Comfort and function remain key factors in upper limb prosthetic abandonment: findings of a scoping review. *Disabil Rehabil Assist Technol*, 1-10. doi:10.1080/17483107.2020.1738567

Subedi, B., & Grossberg, G. T. (2011). Phantom limb pain: mechanisms and treatment approaches. *Pain Res Treat, 2011*, 864605. doi:10.1155/2011/864605

Sulaiman, W., & Gordon, T. (2013). Neurobiology of peripheral nerve injury, regeneration, and functional recovery: from bench top research to bedside application. *Ochsner J. , 13*(1), 100-108.

Swett, J. E., Wikholm, R. P., Blanks, R. H. I., Swett, A. L., & Conley, L. C. (1986). Motoneurons of the Rat Sciatic Nerve. *Experimental Neurology, 93*, 227-252. doi:10.1016/0014-4886(86)90161-5

Tan, D. W., Schiefer, M. A., Keith, M. W., Anderson, J. R., & Tyler, D. J. (2015). Stability and selectivity of a chronic, multi-contact cuff electrode for sensory stimulation in human amputees. *J Neural Eng, 12*(2), 026002. doi:10.1088/1741-2560/12/2/026002

Tan, D. W., Schiefer, M. A., Keith, M. W., Anderson, J. R., Tyler, J., & Tyler, D. J. (2014). A neural interface provides long-term stable natural touch perception. *Sci Transl Med, 6*(257), 257ra138. doi:10.1126/scitranslmed.3008669

Valle, G., Mazzoni, A., Iberite, F., D'Anna, E., Strauss, I., Granata, G., . . . Micera, S. (2018). Biomimetic Intraneural Sensory Feedback Enhances Sensation Naturalness, Tactile Sensitivity, and Manual Dexterity in a Bidirectional Prosthesis. *Neuron, 100*(1), 37-45 e37. doi:10.1016/j.neuron.2018.08.033

Vasudevan, S., Patel, K., & Welle, C. (2017). Rodent model for assessing the long term safety and performance of peripheral nerve recording electrodes. *J Neural Eng, 14*(1), 016008. doi:10.1088/1741-2552/14/1/016008

Verstraelen, P., Van Dyck, M., Verschuuren, M., Kashikar, N. D., Nuydens, R., Timmermans, J. P., & De Vos, W. H. (2018). Image-Based Profiling of Synaptic Connectivity in Primary Neuronal Cell Culture. *Front Neurosci, 12*, 389. doi:10.3389/fnins.2018.00389

Wendelken, S., Page, D. M., Davis, T., Wark, H. A. C., Kluger, D. T., Duncan, C., . . . Clark, G. A. (2017). Restoration of motor control and proprioceptive and cutaneous sensation in humans with prior upper-limb amputation via multiple Utah Slanted Electrode Arrays (USEAs) implanted in residual peripheral arm nerves. *J Neuroeng Rehabil, 14*(1), 121. doi:10.1186/s12984-017-0320-4

Wiedenmann, B., & Franke, W. W. (1985). Identification and Localization of Synaptophysin, an Integral Membrane Glycoprotein of Mr 38,000 Characteristic of Presynaptic Vesicles. *Cell, 41*(3), 1017-1028. doi:10.1016/s0092-8674(85)80082-9

Wurth, S., Capogrosso, M., Raspopovic, S., Gandar, J., Federici, G., Kinany, N., . . . Micera, S. (2017). Long-term usability and bio-integration of polyimide-based intra-neural stimulating electrodes. *Biomaterials, 122*, 114-129. doi:10.1016/j.biomaterials.2017.01.014

Zabaglo, M., & Dreyer, M. A. (2020). Neuroma. Retrieved from https://www.ncbi.nlm.nih.gov/books/NBK549838/

Ziegler-Graham, K., MacKenzie, E. J., Ephraim, P. L., Travison, T. G., & Brookmeyer, R. (2008). Estimating the prevalence of limb loss in the United States: 2005 to 2050. *Arch Phys Med Rehabil, 89*(3), 422-429. doi:10.1016/j.apmr.2007.11.005

Zollo, L., Di Pino, G., Ciancio, A. L., Ranieri, F., Cordella, F., Gentile, C., . . . Guglielmelli, E. (2019). Restoring tactile sensations via neural interfaces for real-time force-and-slippage closed-loop control of bionic hands. *Science Robotics, 4*(27), eaau9924. doi:10.1126/scirobotics.aau9924

Appendix

A)

Condition	Region	n	Avg puncta nb	% beads with one puncta
CTRL 4 wks	distal	41	1.32	68%
	crush	37	1.11	65%
PDL 4 wks	distal	62	1.35	68%
	crush	51	1.49	76%
DND 4 wks	distal	85	1.95	87%
	crush	70	1.74	87%

B)

Condition	Region	n	Avg puncta nb	% beads with one puncta
CTRL 6 wks	distal	105	1.5	69%
	crush	66	1.67	76%
PDL 6 wks	distal	46	2.43	87%
	crush	50	1.94	82%
DND 6 wks	distal	89	2.63	87%
	crush	102	2.73	87%

C)

Condition	Region	n	Avg puncta nb	% beads with one puncta
CTRL 8 wks	distal	55	1.4	65%
	crush	53	2.45	87%
PDL 8 wks	distal	32	2	78%
	crush	14	1.71	79%
DND 8 wks	distal	24	2.58	83%
	crush	19	1.74	84%

Tableau 1. – Raw data values for the average number of synaptophysin puncta on microbeads and the percentage of microbeads with one synaptophysin puncta or more for the experimental conditions CTRL, PDL and DND at the time points: A) 4 weeks, B) 6 weeks and C) 8 weeks

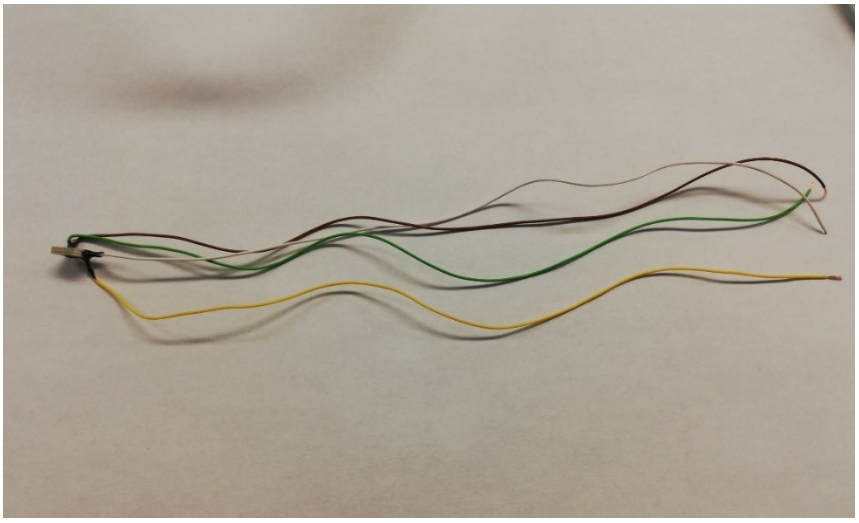

Figure 11. – Implant design for the uncoated electrodes used in the uncoated electrode in vivo experiment. Green: recording electrode; Yellow: stimulation electrode; White: ground electrode; Brown: reference electrode; White: headstage connector.

A) **B)**

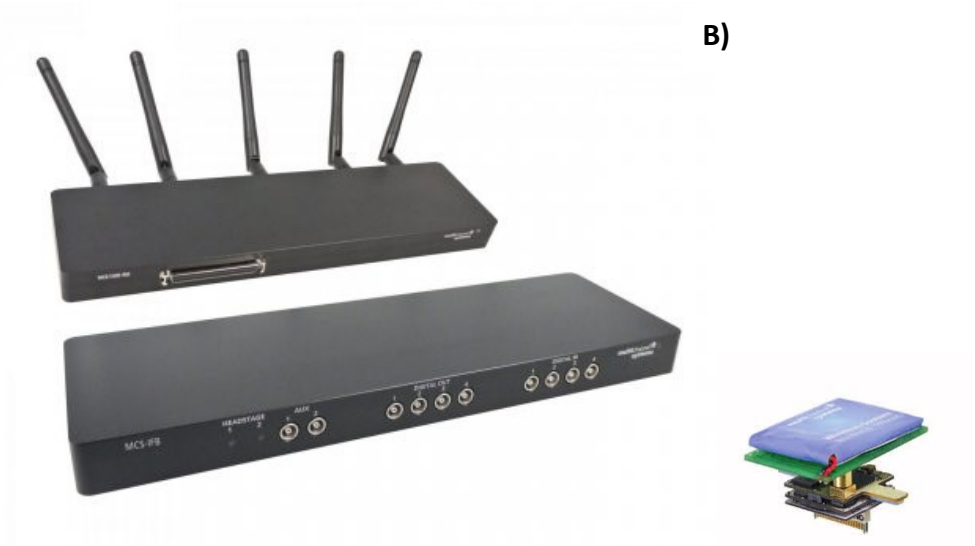

Figure 12. – Representative image of A) the wireless data acquisition system (Multichannel W2100 System) and B) the headstage used for the electrophysiological stimulations and recordings in the uncoated electrode in vivo experiment.